Adv Polym Sci (2011) 238: 1–66
DOI: 10.1007/12_2010_84

Published online: 13 July 2010

Making Flory–Huggins Practical: Thermodynamics of Polymer-Containing Mixtures

Bernhard A. Wolf

Abstract The theoretical part of this article demonstrates how the original Flory–Huggins theory can be extended to describe the thermodynamic behavior of polymer-containing mixtures quantitatively. This progress is achieved by accounting for two features of macromolecules that the original approach ignores: the effects of chain connectivity in the case of dilute solutions, and the ability of polymer coils to change their spatial extension in response to alterations in their molecular environment. In the general case, this approach leads to composition-dependent interaction parameters, which can for most binary systems be described by means of two physically meaningful parameters; systems involving strongly interacting components, for instance via hydrogen bonds, may require up to four parameters. The general applicability of these equations is illustrated in a comprehensive section dedicated to the modeling of experimental findings. This part encompasses all types of phase equilibria, deals with binary systems (polymer solutions and polymer blends), and includes ternary mixtures; it covers linear and branched homopolymers as well as random and block copolymers. Particular emphasis is placed on the modeling of hitherto incomprehensible experimental observations reported in the literature.

Keywords Modeling · Mixed solvents · Phase diagrams · Polymer blends · Polymer solutions · Ternary mixtures · Thermodynamics

B.A. Wolf
Institut für Physikalische Chemie der Johannes Gutenberg-Universität Mainz, 55099 Mainz, Germany
e-mail: bernhard.wolf@uni-mainz.de

Contents

Symbols

a	Exponent of Kuhn–Mark–Houwink relation (29)
a	Intramolecular interaction parameter (47) for blend component A
A,B,C	Constants of (13)
A_2, A_3	Second and third osmotic virial coefficients
a_i	Activity of component i
b	Intramolecular interaction parameter (47) for blend component B
c	Concentration in moles/volume
E	Constant of interrelating α and $\zeta\lambda$ (34)
G	Gibbs free energy – free enthalpy
g	Integral interaction parameter
H	Enthalpy
K_N	Constant of the Kuhn–Mark–Houwink relation (29)
LCST	Lower critical solution temperature
M	Molar mass
M_n	Number-average molar mass
M_w	Weight-average molar mass
N	Number of segments
n	Number of moles
p	Vapor pressure
R	Ideal gas constant
S	Entropy
s	Molecular surface
T	Absolute temperature
t	Ternary interaction parameter (61)
T_m	Melting point
UCST	Upper critical solution temperature
V	Volume
v	Molecular volume

w	Weight fraction
x	Mole fraction
Z	Parameter relating the conformational relaxation to β (53)

Greek and Special Characters

$\overline{\omega}$	Parameter quantifying strong intersegmental interactions (42)
$[\eta]$	Intrinsic viscosity
Φ_o	Volume fraction of polymer segments in an isolated coil (27)
Θ	Theta temperature
α	Parameter of (23), first step of dilution
β	Degree of branching (52)
χ	Flory–Huggins interaction parameter
δ	Parameter of (57)
ε	Parameter of (57)
γ	Surface-to-volume ratio of the segments in binary mixtures (24)
φ	Segment fraction, often approximated by volume fraction
κ	Constant of (30)
λ	Intramolecular interaction parameter (23)
μ	Chemical potential
ν	Parameter of (23)
π	Any parameter of (23)
π_{osm}	Osmotic pressure
ρ	Density
τ	Parameter of (44)
ξ	Differential Flory–Huggins interaction parameter for the polymer
ζ	Conformational relaxation (second step of dilution) (23)

Subscripts

1, 2, 3 ...	Low molecular weight components of a mixture
A to P	High molecular weight components
B	Branched oligomer/polymer
c	Critical state
cr	Conformational relaxation
fc	Fixed conformation
g	Glass
H	Enthalpy part of a parameter
i, j, k	Unspecified components i, j, k
L	Linear polymer
lin	Linear oligomer/polymer
m	Melting
S	Entropy part of a parameter

s	Saturation
o	Quantity referring to a pure component, to an isolated coil, or to high dilution

Superscripts

–	Molar quantity
=	Segment-molar quantity
E	Excess quantity
Res	Residual quantity (with respect to combinatorial behavior)
∞	Infinite molar mass of the polymer

1 Introduction

The decisive advantage of the original Flory–Huggins theory [1] lies in its simplicity and in its ability to reproduce some central features of polymer-containing mixtures qualitatively, in spite of several unrealistic assumptions. The main drawbacks are in the incapacity of this approach to model reality in a quantitative manner and in the lack of theoretical explanations for some well-established experimental observations. Numerous attempts have therefore been made to extend and to modify the Flory–Huggins theory. Some of the more widely used approaches are the different varieties of the lattice fluid and hole theories [2], the mean field lattice gas model [3], the Sanchez–Lacombe theory [4], the cell theory [5], different perturbation theories [6], the statistical-associating-fluid-theory [7] (SAFT), the perturbed-hard-sphere chain theory [8], the UNIFAC model [9], and the UNIQUAC [10] model. More comprehensive reviews of the past achievements in this area and of the applicability of the different approaches are presented in the literature [11, 12].

This contribution demonstrates how the deficiencies of the original Flory–Huggins theory can be eliminated in a surprisingly simple manner by (1) accounting for hitherto ignored consequences of chain connectivity, and (2) by allowing for the ability of macromolecules to rearrange after mixing to reduce the Gibbs energy of the system. Section 2 recalls the original Flory–Huggins theory and describes the composition dependence of the Flory–Huggins interaction parameters resulting from the incorporation of the hitherto neglected features of polymer/solvent systems into the theoretical treatment. This part collects all the equations required for the interpretation of comprehensive literature reports on experimentally determined thermodynamic properties of polymer-containing binary and ternary mixtures (polymer solutions in mixed solvents and solutions of two polymers in a common solvent). In order to ease the assignment of the different variables and parameters to a certain component, the low molecular weight components are identified by numbers and the polymers by letters. The high molecular weight components comprise linear and branched samples, homopolymers, binary random copolymers,

and block copolymers of different architecture; the phase equilibria encompass liquid/gas, liquid/liquid and liquid/solid. The only aspects that are excluded are the coexistence of three liquid phases and the demixing of mixed solvent.

This theoretical section is followed (Sect. 3) by a recap of the measuring techniques used for the determination of the thermodynamic properties discussed here. The subsequent main part of the article (Sect. 4) outlines the modeling of experimental observations and investigates the predictive power of the extended Flory–Huggins theory. Throughout this contribution, particular attention is paid to phenomena that cannot be rationalized on the basis of the original Flory–Huggins theory, like anomalous influences of molar mass on thermodynamic properties or the existence of two critical points (liquid/liquid phase separation) for binary systems. In fact, it was the literature reports on such experimental findings that have prompted the present theoretical considerations.

2 Extension of the Flory–Huggins Theory

2.1 Binary Systems

2.1.1 Polymer Solutions

Organic Solvents/Linear Homopolymers

The basis for a better understanding of the particularities of polymer-containing mixtures as compared with mixtures of low molecular weight compounds was laid more than half a century ago [13–17], in the form of the well-known Flory–Huggins interaction equation. By contrast to the form used for low molecular weight mixtures, this relation is usually not stated in terms of the *molar* Gibbs energy $\overline{G}$; for polymer-containing systems one chooses one mole of segments as the basis (in order to keep the amount of matter under consideration of the same order of magnitude) and introduces the *segment molar* Gibbs energy $\overline{\overline{G}}$. For polymer solutions, where the molar volume of the solvent normally defines the size of a segment, this relation reads:

$$\frac{\Delta\overline{\overline{G}}}{RT} = (1-\varphi)\ln(1-\varphi) + \frac{\varphi}{N}\ln\varphi + g\varphi(1-\varphi) \tag{1}$$

$\Delta\overline{\overline{G}}$ stands for the segment molar Gibbs energy of mixing. The number N of segments that form the polymer is calculated by dividing the molar volume of the macromolecule by the molar volume of the solvent. The composition variable φ, representing the segment molar fraction of the polymer, is in most cases approximated by its volume fraction (neglecting nonzero volumes of mixing), and g stands for the integral Flory–Huggins interaction parameter. In the case of polymer

solutions, we refrain from using indices whenever possible (i.e., we write g instead of g_{1P}, φ instead of φ_P and N instead of N_P) for the sake of simpler representation. Only if g does not depend on composition does it becomes identical with the experimentally measurable Flory–Huggins interaction parameter χ, introduced in (5).

The total change in the Gibbs energy resulting from the formation of polymer solutions is, according to (1), subdivided into two parts, the first two terms representing the so-called combinatorial behavior, ascribed to entropy changes:

$$\frac{\Delta\overline{\overline{G}}^{\,\mathrm{com}}}{RT} = (1-\varphi)\ln(1-\varphi) + \frac{\varphi}{N}\ln\varphi \tag{2}$$

All particularities of a certain real system (except for the chain length of the polymer) are incorporated into the third term, the residual Gibbs energy of mixing, and were initially considered to be of enthalpic origin. The essential parameter of this part is g, the integral Flory–Huggins interaction parameter:

$$\frac{\Delta\overline{\overline{G}}^{\,\mathrm{res}}}{RT} = g\varphi(1-\varphi) \tag{3}$$

In the early days, the Flory–Huggins interaction parameter was considered to depend only on the variables of state, but not on either the composition of the mixture or on the molar mass of the polymer. Under these premises, it is easy to perform model calculations – for instance with respect to phase diagrams – along the usual routes of phenomenological thermodynamics on the sole basis of the parameter g. In this manner, most characteristic features of polymer solutions can already be well rationalized, even though quantitative agreement is lacking. However, as the number of thermodynamic studies increased it was soon realized that (1) is too simple. Above all, it became clear that the assignment of entropy and of enthalpy contributions to the total Gibbs energy of mixing is unrealistic. Maintaining for practical reasons the first term unchanged, as a sort of reference behavior, this means that all particularities of a real system must be incorporated into the parameter g.

This change in strategy has important consequences, the most outstanding being the necessity to distinguish between *integral* interaction parameters g, introduced by (1) and referring to the Gibbs energy of mixing, and *differential* interaction parameters, referring either to the chemical potential of the solvent or of the solute. The partial segment molar Gibbs energies and the corresponding integral quantity are interrelated by the following relation:

$$\overline{\overline{G}}_i = \overline{\overline{G}} - \varphi_k \frac{\partial\overline{\overline{G}}}{\partial\varphi_k} \tag{4}$$

where the subscripts i and k stand for either the solvent or the polymer. The partial molar Gibbs energies $\overline{G}_i$ are customary referred to as chemical potentials μ_i.

The partial expressions for the solvent (index 1) read:

$$\frac{\Delta\mu_1}{RT} = \frac{\Delta\overline{\overline{G}}_1}{RT} = \ln(1-\varphi) + \left(1 - \frac{1}{N}\right)\varphi + \chi\,\varphi^2 = \ln\, a_1 \tag{5}$$

and yield the differential parameter χ, the well known original Flory–Huggins interaction parameter, which is related to the activity a_1 of the solvent as formulated above; a_1 can in many cases be approximated (sufficiently low volatility of the solvent) by the relative vapor pressure:

$$a_1 \approx \frac{p_1}{p_{1,\mathrm{o}}} \tag{6}$$

where $p_{1,\mathrm{o}}$ is the vapor pressure of the pure solvent. Otherwise, one needs to correct for the imperfections of the equilibrium vapor.

The Flory–Huggins interaction parameter constitutes a measure for chemical potential of the solvent, as documented by (6) and (5); it is defined in terms of the deviation from combinatorial behavior as:

$$\chi \equiv \frac{\Delta\overline{\overline{G}}_1^{\mathrm{res}}}{RT\varphi^2} \tag{7}$$

In the original theory, χ was meant to have an immediate physical meaning, because of the normalization of the residual segment molar Gibbs energies of dilution to the probability φ^2 of an added solvent molecule to be inserted between two contacting polymer segments. This illustrative interpretation does, however, rarely hold true in reality. Even for simple homopolymer solutions in single solvents, it fails in the region of high dilution because the overall polymer concentration becomes meaningless for the number of intermolecular contacts between polymer segments. Despite this lack of a straightforward interpretation of the Flory–Huggins interaction parameter in molecular terms, the knowledge of $\chi(\varphi)$ is indispensable for the thermodynamic description of polymer-containing mixtures. This information can be converted to integral interaction parameters g [cf. (25)] and gives access to the calculation of macrophase separation (e.g., via a direct minimization of the Gibbs energy of the systems [18–20] and to the chemical potentials of the polymer [cf. (11)].

For practical purposes, the use of volume fractions (instead of the original segment fractions) as composition variable is not straightforward because of the necessity to know the densities of the components and (in the case of variable temperature) their thermal expansivities. For that reason, φ is sometimes consistently replaced by the weight fraction w, and N calculated from the molar masses as M_{P}/M_1. The χ values obtained in this manner according to (8):

$${}_w\chi \equiv \frac{{}_{\mathrm{w}}\Delta\overline{\overline{G}}_1^{\mathrm{res}}}{RTw^2} \tag{8}$$

are indicated by the subscript w and may differ markedly in their numerical values from χ. The expression for the residual Gibbs energy of dilution is also given an index as a reminder that weight fractions were used to calculate its combinatorial part. Despite the practical advantages of ${}_w\chi$, we stay with volume fractions for all subsequent considerations, because they account at least partly for the differences in the free volume of the components and because most of the published thermodynamic information uses this composition variable.

One of the consequences of composition-dependent interaction parameters lies in the necessity to distinguish between different parameters, depending on the particular method by which they are determined. The Flory–Huggins interaction parameter χ relates to the integral interaction parameter g as:

$$\chi = g - (1-\varphi)\,\frac{\partial g}{\partial \varphi} \tag{9}$$

The expression analogous to (5), referring to the solvent, reads for the polymer (index P):

$$\frac{\Delta\mu_{\mathrm{P}}}{RT} = \frac{N\,\Delta\overline{\overline{G}}_{\mathrm{P}}}{RT} = \ln\varphi + (1-N)(1-\varphi) + \xi N(1-\varphi)^2 \tag{10}$$

This relation defines the differential interaction parameter ξ in terms of the chemical potential of the polymer and is calculated from g by means of:

$$\xi = g + \varphi\frac{\partial g}{\partial \varphi} \tag{11}$$

Out of the three types of interaction parameters, it is almost exclusively χ that is of relevance for the thermodynamic description of binary and ternary polymer-containing liquids, as will be described in the section on experimental methods (Sect. 3). The integral interaction g parameter is practically inaccessible, and the parameter ξ, referring to the polymer, suffers from the difficulties associated with the formation of perfect polymer crystals, because it is based on their equilibria with saturated polymer solutions.

Measured Flory–Huggins interaction parameters soon demonstrated the necessity to treat χ as composition-dependent. A simple mathematical description consists of the following series expansion:

$$\chi = \chi_{\mathrm{o}} + \chi_1\varphi + \chi_2\varphi^2 \ldots \tag{12}$$

A more sophisticated approach [21] accounts for the differences in the molecular surfaces of solvent molecules and polymer segments (of equal volume) and formulates $\chi(\varphi)$ as:

$$\chi = \frac{A}{(1 - B\varphi)^2} + C \tag{13}$$

where these differences are contained in the parameter B. A and C are considered to be further constants for a given system and fixed variables of state.

The thermodynamic relations discussed so far were, above all, formulated for the description of moderately to highly concentrated polymer solutions. The information acquired in the context of the determination of molar masses, on the other hand, refers to dilute solution and is usually expressed in terms of second osmotic virial coefficients A_2 and higher members of a series expansion of the chemical potential of the solvent with respect to the polymer concentration c (mass/volume). For the determination of osmotic pressures, π_{osm}, the corresponding relation reads:

$$-\frac{\Delta\bar{G}_1}{RT\,\overline{V}_1} = \frac{\pi_{\mathrm{osm}}}{RT} = \frac{c}{M_{\mathrm{n}}} + A_2 c^2 + A_3 c^3 + \ldots \tag{14}$$

Performing a similar series expansion for the logarithm in (5), inserting χ from (12) into this relation, and comparing the result with (14) yields [21]:

$$\chi_{\mathrm{o}} = \frac{1}{2} - \rho_{\mathrm{P}}^2\,\overline{V}_1\,A_2 \tag{15}$$

and:

$$\chi_1 = \frac{1}{3} - \rho_{\mathrm{P}}^3\,\overline{V}_1\,A_3 \tag{16}$$

where χ_{o} represents the Flory–Huggins interaction parameter in the limit of pair interactions between polymer molecules. $\overline{V}_1$ is the molar volume of the solvent and ρ_{P} is the density of the polymer.

The need for a different view on the thermodynamics of polymer solutions became, in the first place, obvious from experimental information on dilute systems. According to the original Flory–Huggins theory, the second osmotic virial coefficient should without exception decrease with rising molar mass of the polymer. It is, however, well documented (even in an early work by Flory himself [22]) that the opposite dependence does also occur. Based on this finding and on the fact that the Flory–Huggins theory only accounts for chain connectivity in the course of calculating the combinatorial entropy of mixing and for concentrated solutions, we attacked the problem by starting from the highly dilute side.

The central idea of this approach is the treatment of a swollen isolated polymer coil – surrounded by a sea of pure solvent – as a sort of microphase and applying the usual equilibrium condition to such a system. In a thought experiment, one can insert a single totally collapsed polymer molecule into pure solvent and let it swell

until it reaches its equilibrium size. Traditionally, the final state of this process is discussed in terms of chain elasticity. Here, we apply a phenomenological thermodynamic method and equate the chemical potential of the solvent inside the realm of the polymer coil to the chemical potential of the pure solvent surrounding it. In doing so, we "translate" the entropic barrier against an infinite extension of the polymer chain into a virtual semi-permeable membrane. This barrier accounts for chain connectivity and represents a consequence of the obvious inability of the segments of an isolated polymer molecule to spread out over the entire volume of the system. The condition for the establishment of such a microphase equilibrium reads:

$$\ln(1-\Phi_o)+\left(1-\frac{1}{N}\right)\Phi_o+\lambda\Phi_o^2=0 \tag{17}$$

This relation differs from that for macroscopic phase equilibria [resulting from (5)] only by the meaning of the concentration variable Φ_o and of the interaction parameter λ. Φ_o stands for the average volume fraction of the polymer segments contained in an isolated coil, and λ represents an intramolecular interaction parameter, which raises the chemical potential of the solvent in the mixed phase up to the value of the pure solvent.

By means of the considerations outlined above, we have accounted for chain connectivity. However, there is another aspect that the original Flory–Huggins theory ignores, namely the ability of chain molecules to react to changes in their environment by altering their spatial extension. One outcome of this capability is, for instance, the well-known fact that the unperturbed dimensions of pure polymers in the melt will gradually increase upon the addition of a thermodynamically favorable solvent. These changes are particularly pronounced in the range of high dilution, where there is no competition of different solute molecules for available solvent, due to the practically infinite reservoir of pure solvent.

In order to incorporate both features neglected by the original Flory–Huggins theory into the present approach, we have conceptually subdivided the dilution process into two separate steps as formulated in (18). Such a separation is permissible because the Gibbs energy of dilution represents a function of state.

$$\chi_o=\chi_o^{fc}+\chi_o^{cr} \tag{18}$$

The first term (the superscript fc stands for fixed conformation) quantifies the effect of separating two contacting polymer segments belonging to different macromolecules by inserting a solvent molecule between them without changing their conformation. The second term (the superscript cr stands for conformational relaxation) is required to bring the system into its equilibrium by rearranging the components such that the minimum of Gibbs energy is achieved.

In order to give the second term a more specific meaning, we formulate χ_o^{cr} as the difference in the interaction before and after the conformational relaxation as:

$$\chi_o^{cr} = \chi^{after} - \chi^{before} \tag{19}$$

Choosing λ, the interaction between polymer segments and solvent molecules in the isolated state, as a clear cut reference point for the contribution of the rearrangement in the second step of dilution, and assuming that the effect will be proportional to λ, we can write:

$$\chi_o^{cr} = -\zeta\lambda \tag{20}$$

where the negative sign in the above expression has been chosen to obtain positive values for this parameter in the great majorit of cases. Denoting:

$$\chi_o^{fc} = \alpha \tag{21}$$

(18) and (20) yield the following simple expression for the Flory–Huggins interaction parameter in the limit of high dilution:

$$\chi_o = \alpha - \zeta\lambda \tag{22}$$

For sufficiently dilute polymer solutions, the only difference between the new approach and the original Flory–Huggins theory is in the second term. According to theoretical considerations and in accord with experimental findings, ζ becomes zero under theta conditions (where the coils assume their unperturbed dimensions) and the conformational relaxation no longer contributes to χ_o.

In order to generalize (22) to arbitrary polymer concentrations, we assume that the composition dependence of its first term can be formulated by analogy to (13). The necessity of a composition dependence for the second term results from the fact that the insertion of a solvent molecule between contacting polymer segments (belonging to different polymer chains) opens only one binary contact within the composition range of pair interactions, whereas there are inevitably more segments affected at higher polymer concentrations. For the second term, we suppose a linear dependence of the integral interaction parameter g on φ. Comparing the coefficients of this ansatz (as they appear in the expression for differential interaction parameter) with (22) for χ_o results in (23):

$$\chi = \frac{\alpha}{(1 - v\varphi)^2} - \zeta(\lambda + 2(1 - \lambda)\varphi) \tag{23}$$

The symbol v instead of B (13) in the above relation indicates that this parameter is related to γ [21], the geometrical differences of solvent molecules and polymer segments as formulated in the next equation, but not identical with γ;

$$\gamma \equiv 1 - \frac{(s/v)_{polymer}}{(s/v)_{solvent}} \tag{24}$$

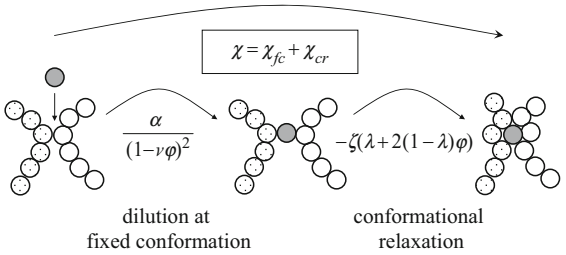

Fig. 1 Assignment of the parameters of (23) to the individual steps of dilution: Two contacting segments belonging to different macromolecules are separated by the insertion of a solvent molecule (*shaded*) between them

The parameters s and v are the molecular surfaces and volumes of the components, respectively. In the limit of $\varphi \to 0$, (23) reduces to (22).

The essentials of the considerations concerning the composition dependence of the Flory–Huggins interaction parameter are visualized in Fig. 1, demonstrating how the dilution is conceptually divided into two separate steps and how these steps contribute to the overall effect. The first step maintains the conformation of the components as they are prior to dilution and does not change the volume of the system; measurable excess volumes are attributed to the conformational rearrangement taking place during the second step of mixing.

By means of the expression:

$$g = -\frac{1}{1-\varphi}\int_{1}^{1-\varphi} \chi \, \mathrm{d}\,\varphi \tag{25}$$

resulting from phenomenological thermodynamics, the Flory–Huggins interaction parameter χ of (23) yields the following expression for the integral interaction parameter g, required for instance to calculate phase equilibria using the method of the direct minimization of the Gibbs energy [19] of a system:

$$g = \frac{\alpha}{(1-v)\,(1-v\varphi)} - \zeta(1+(1-\lambda)\varphi) \tag{26}$$

This relation contains four adjustable parameters; even if they are molecularly justified these are too many for practical purposes. For this reason, it would be helpful to be able to calculate at least one of them independently. The most obvious candidate for that purpose is λ (17) because it refers to the spatial extension of isolated polymer coils. Radii of gyration would be most qualified for calculation of the required volume fractions of segments, Φ_o, inside the microphase formed by isolated polymer molecules. Unfortunately, however, it is hard to find tabulated values for different polymer/solvent systems in the literature. For this reason, we use information provided by the specific hydrodynamic volume of the polymers at infinite dilution, i.e., to intrinsic viscosities $[\eta]$. The volume of the segments is

given by M/ρ_P, and $[\eta]M$ yields the hydrodynamic volume of one mole of isolated polymer coils so that Φ_o becomes:

$$\Phi_o = \frac{M/\rho_P}{[\eta]M} = \frac{1}{[\eta]\rho_P} \tag{27}$$

Upon the expansion of the logarithm in (17) up to the second term (which suffices in view of the low Φ_o values typical for the present systems), we obtain the following expression for λ:

$$\lambda = \frac{1}{2} + \frac{[\eta]\rho_P}{N} \tag{28}$$

Relating the intrinsic viscosity to N by means of the Kuhn–Mark–Houwink relation:

$$[\eta] = K_N N^a \tag{29}$$

the intramolecular interaction parameter becomes:

$$\lambda = \frac{1}{2} + \kappa N^{-(1-a)} \tag{30}$$

where $\kappa = K_N \rho_P$.

The insertion of (30) into (22) and employing (15) enables the rationalization of the experimental finding that the A_2 values for the solutions of a given polymer of different chain length do not exclusively decrease with rising M in good solvents, but might also increase. The resulting equation reads:

$$A_2 = A_2^\infty + \frac{\zeta\kappa}{\rho_P^2 \overline{V}} N^{-(1-a)} \tag{31}$$

where A_2^∞ is the limiting value of A_2 for infinite molar mass of the polymer. The reason for an anomalous molecular weight dependence of the second osmotic virial coefficient lies in the sign of ζ, which is positive in most cases, but may also become negative under special conditions. For theta systems, $A_2 = 0$, irrespective of M, and ζ becomes zero. One consequence of the present experimentally verified consideration concerns the way that $A_2(M)$ should be evaluated. Equation (31) requires plots of A_2 as a function of $M^{-(1-a)}$, instead of the usual double logarithmic plots, and does not – in contrast to the traditional evaluation – automatically yield zero second osmotic virial coefficient in the limit of infinitely long chains.

Another helpful consequence of (30) lies in the fact that its second term is almost always negligible (with respect to 1/2) for polymers of sufficient molar mass. This feature allows the merging of the parameters ζ and λ into their product $\zeta\lambda$, and the

replacement of the isolated λ by 1/2, as formulated below for the differential interaction parameter χ:

$$\chi \approx \frac{\alpha}{(1-v\varphi)^2} - \zeta\lambda(1+2\varphi) \tag{32}$$

The analogous relation for the integral interaction parameter reads:

$$g \approx \frac{\alpha}{(1-v)\,(1-v\varphi)} - \zeta\lambda(2+\varphi) \tag{33}$$

By this means, the number of adjustable parameter reduces to three. As will be shown in the section dealing with experimental data (Sect. 4), further simplifications are possible, for instance because of a theoretically expected interrelation between the parameters α (first step of mixing) and $\zeta\lambda$ (second step of mixing) for a given class of polymer solutions. In its general form this equation reads:

$$\zeta\lambda = E(2\,\alpha - 1) \tag{34}$$

where E is a constant, typically assuming values between 0.6 and 0.95. Equation (34) is in accord with the typical case of theta conditions where $\zeta \to 0$ and $\alpha \to 0.5$. As long as such an interrelation exists, the number of parameters required for the quantitative description of the isothermal behavior of polymer solutions reduces to two. Like with the expression for χ_o (high dilution), the contributions of chain connectivity and conformational relaxation are in (32) (arbitrary polymer concentration) exclusively contained in the second term. Another aspect also deserves mentioning, namely the fact that (32) is not confined to the modeling of polymer-containing systems but can also be successfully applied to mixtures of low molecular weight liquids, as will be shown in Sect. 4.

According to expectation, and in agreement with measurements, all system-specific parameters π (namely α, v, ζ, and λ) vary more or less with temperature (and pressure). The following relation is very versatile to model $\pi(T)$:

$$\pi = \pi_o + \frac{\pi_1}{T} + \pi_2 T \tag{35}$$

where either π_1 or π_2 can be set to zero in most cases.

Up to now, it was the chemical potential of the solvent that constituted the object of prime interest. The last part of this section is dedicated to the modeling of liquid/liquid phase separation by means of the integral Gibbs energy of mixing in the case of polymer solutions. The equations presented in this context can, however, be easily generalized to polymer blends and to multinary systems. Such calculations are made possible by using the minimum Gibbs energy a system can achieve via phase separation as the criterion for equilibria, instead of equality of the chemical potentials of the components in the coexisting phases. The method of a direct

minimization of the Gibbs energy [19] works in the following way: The segment molar Gibbs energy of mixing for the (possibly unstable) homogeneous system is calculated by means of (1), where the integral interaction parameter g is in the present case taken from (26). For different overall compositions, it is then checked on a computer by means of test tie lines (connecting arbitrarily chosen data points of the function $\Delta\overline{\overline{G}}$) which values lead to the maximum lowering of the Gibbs energy. In this manner, it is possible to model the binodal curves if $g(T)$ is known. Spinodal curves are also easily accessible by means of these test tie lines, if they are chosen to be very short. In this manner, it is possible to monitor at which concentration the test tie lines change their location with respect to the function $\Delta\overline{\overline{G}}/RT(\varphi)$: Within the unstable range they lie below that function, and within the metastable and stable ranges they are located above it, indicating that homogenization would lead to a further reduction in G. The criterion that (sufficiently short) test tie lines must become parallel to the spinodal line at the critical point gives access to critical data.

Under special conditions, it possible to calculate system-specific parameters from experimentally determined critical concentrations φ_c. The condition for the degeneration of the tie lines to the critical point is that the second and the third derivative of the Gibbs energy with respect to composition must become zero. The application of this requirement to (1) in combination with (26) yields:

$$\frac{1}{1-\varphi_c}+\frac{1}{N\varphi_c}+\frac{2\alpha}{(v\varphi_c-1)^3}+2\zeta[\lambda-3\varphi_c(\lambda-1)]=0 \tag{36}$$

and:

$$\frac{1}{(\varphi_c-1)^2}-\frac{1}{N\varphi_c^2}-\frac{6\alpha v}{(v\varphi_c-1)^4}+6\zeta(1-\lambda)=0 \tag{37}$$

For the sake of completeness, the coexistence of a pure crystalline polymer with its saturated solution is also considered. Taking the change in the chemical potential of the polymer upon mixing from (10), the equilibrium condition ($T \leq T_m$) reads:

$$\Delta\overline{\overline{H}}_m-T\frac{\Delta\overline{\overline{H}}_m}{T_m}+RT\left(\ln\varphi_s+(1-N)\varphi_s+N_P\xi(1-\varphi_s)^2\right)=0 \tag{38}$$

where the entropy term of the segment molar Gibbs energy of melting [the second term of (38)] is approximated by $\Delta\overline{\overline{H}}_m$, the segment molar heat of melting, and the melting temperature T_m of the pure crystal; φ_s denotes the saturation volume fraction of the polymer in the solution.

So far, we have not dealt with the question of how the Flory–Huggins interaction parameters are made up of enthalpy and entropy contributions for different systems. This information is accessible by means of (39) and (40) (which neglect the

temperature influences on the volume fraction of the polymer, caused by different thermal expansivities of the components). The enthalpy part reads:

$$\chi_H = -T\left(\frac{\partial\chi}{\partial T}\right)_{\mathrm{p}} \tag{39}$$

and the corresponding entropy part is given by:

$$\chi_S = \chi + T\left(\frac{\partial\chi}{\partial T}\right)_{\mathrm{p}} \tag{40}$$

In the above equations, χ can be substituted by any parameter of the present approach to determine its enthalpy and entropy parts, except for the parameter v, which is not a Gibbs energy by its nature.

Organic Solvents/Branched Homopolymers

The different molecular architectures of branched polymers do not require modifications of (32); the particularities of branched polymers only change the values of the system-specific parameters as compared with those for linear analogs in the same solvent [24], as intuitively expected.

Organic Solvents/Linear Random Copolymers

Despite the fact that these solutions represent binary systems, at least three Flory–Huggins interaction parameters are involved in their modeling, like with ternary mixtures. Because of the necessity to account for the interaction of the solvent with monomer A and with monomer B, plus the interaction between the polymers A and B, one should expect the need for a minimum of two additional parameters. Experimental data obtained for solutions of a given copolymer of the type A-ran-B with a constant fraction f of B monomers can be modeled [25] by means of (32), with one set of α, v, and $\zeta\lambda$ parameters. For predictive purposes, it would of course be interesting to find out how these parameters for the copolymer solution (subscripts AB) relate to the parameters for the solutions of the corresponding homopolymers in the same solvent (subscripts A and B, respectively) at the same temperature.

Measured composition-dependent interaction parameters [25] for solutions of the homopolymers poly(methyl methacrylate) (PMMA) and polystyrene (PS) in four solvents on one hand, and for the corresponding solutions of random

copolymers with different weight fractions f of styrene units on the other hand, are well modeled by the following relation:

$$\pi_{AB} = \pi_A(1-f) + \pi_B f + \pi^E f(1-f) \tag{41}$$

in which π stands for the different system-specific parameters α, v, and $\zeta\lambda$. Experimental data indicate [25] that the contribution of the excess term π^E might become negligible for one of the three parameters α, v, or $\zeta\lambda$, but not for the other two.

Polymer Solutions: Special Interactions

The common feature of one group of systems that deviate from normal behavior lies in the solvent, water. The present examples refer to mixtures of polysaccharides and water, which cannot be modeled in the usual manner. Aqueous solutions of poly (vinyl methyl ether) (PVME), exhibiting a second critical concentration, fall into the same category. Solutions of block copolymers in a nonselective solvent represent another instance of the need to extend the approach beyond the state formulated in (32).

Water/Polysaccharides

For the systems characterized by strong interactions between two monomeric units via hydrogen bonds, it is necessary to account for the energy of these very favorable contacts when inserting a solvent molecule between them in the first step of mixing (the parameter α is too unspecific to account for that particularity). This idea has lead to the following extension [26] of (26) for the integral interaction parameter:

$$g = \frac{\alpha}{(1-v)(1-v\varphi)} - \zeta(1 + (1-\lambda)\varphi) + \overline{\omega}\,\varphi^2 \tag{42}$$

where the quadratic term in φ is due to the fact that only two macromolecules are involved in the formation of such energetically preferred intersegmental contacts; $\overline{\omega}$ quantifies the strength of these interactions.

The corresponding expression for χ [obtained according to (9)] reads:

$$\chi = \frac{\alpha}{(1-v\varphi)^2} - \zeta(\lambda + 2(1-\lambda)\varphi) + \overline{\omega}\,\varphi(3\varphi - 2) \tag{43}$$

Comparison of this relation with experimental data demonstrates that the parameters ζ and λ can again be merged without loss of accuracy, as shown in (32).

Organic Solvents/Block Copolymers

This is a further kind of system that cannot be modeled by means of the simple (32), referring to typical homopolymer solutions. Like with aqueous solutions of polysaccharides, the reason lies in special interactions between the segments of the different polymer chains. With block copolymers, the interactions are due to the high preference of contacts between like monomeric units over disparate contacts in cases where the homopolymers are incompatible. There is, however, a fundamental difference, namely in the number of segments that are involved in the formation of the energetically preferred structures. Two units are required for the polysaccharides (two segments are involved in the formation of a hydrogen bond), but with block copolymers of this type the interaction of at least three like monomeric units is on the average indispensable to form a microphase. This is another consequence of chain connectivity. For low molecular weight compounds, the number of nearest neighbor molecules is approximately six in the condensed state. The corresponding number of contacting polymer segments on the other hand is only about half this value, because of the chemical bonds connecting these segments to a chain molecule.

Based on these considerations, postulating the simultaneous interaction of three like segments for the establishment of a microphase, we can formulate the following relation for the integral interaction parameter g, by analogy to (42), increasing the power of the composition dependence of the third term from two to three:

$$g = \frac{\alpha}{(1-v)\,(1-v\varphi)} - \zeta(1 + (1-\lambda)\varphi) + \tau\,\varphi^3 \tag{44}$$

The system-specific parameter τ accounts for the degree of incompatibility of homopolymer A and homopolymer B.

Equation (44) yields, by means of (9), the following expression for the experimentally accessible Flory–Huggins interaction parameter χ:

$$\chi = \frac{\alpha}{(1-v\varphi)^2} - \zeta(\lambda + 2(1-\lambda)\varphi) + \tau\,\varphi^2(4\,\varphi - 3) \tag{45}$$

Like with normal polymer solutions, it is also possible to merge ζ and λ for solutions of block copolymers, i.e., to eliminate one adjustable parameter.

2.1.2 Polymer Blends

For mixtures of two types of linear chain molecules, A and B, the segment molar Gibbs energy of mixing is usually formulated as:

$$\frac{\Delta\overline{\overline{G}}_{AB}}{RT} = \frac{(1-\varphi_B)}{N_A}\ln(1-\varphi_B) + \frac{\varphi_B}{N_B}\ln\varphi_B + g_{AB}\varphi_B(1-\varphi_B) \tag{46}$$

where N_A is the number of segments of component A and N_B is the number of segments of component B. The above equation shows the indices of the variables and parameters to indicate that it refers to a polymer blend. For such systems, the definition of a segment is not as evident as for polymer solutions, where the solvent usually fixes its volume. Sometimes the monomeric unit of one of the components is chosen to specify a segment, but in most cases it is arbitrarily defined as 100 mL per mole of segments, a choice that eases the comparison of the degrees of incompatibility for different polymer pairs.

In the case of polymer solutions, only one component of the binary mixtures suffers from the restrictions of chain connectivity, namely the macromolecules, whereas the solvent can spread out over the entire volume of the system. With polymer blends this limitations of chain connectivity applies to both components. In other words: Polymer A can form isolated coils consisting of one macromolecule A and containing segments of many macromolecules B and vice versa. This means that we need to apply the concept of microphase equilibria twice [27] and require two intramolecular interaction parameters to characterize polymer blends, instead of the one λ in case of polymer solutions.

The conditions for the establishment of microphase equilibria in the case of polymer blends [27], analogous to (17) for polymer solutions, yields two parameters. One, called a, quantifies the restrictions of the segments of a given polymer B to mix with the infinite surplus of A segments surrounding its isolated coil (microphase equilibrium for component A) and an analogous parameter b, referring to the restrictions of the segments of a given polymer A to mix with the infinite surplus of B segments. The following relations hold true for a and b:

$$a = \frac{1}{2N_A} + \frac{1}{N_B \Phi_{o,B}} \tag{47}$$

and:

$$b = \frac{1}{2N_B} + \frac{1}{N_A \Phi_{o,A}} \tag{48}$$

where the Φ values are volume fractions of segments in isolated coils, by analogy to those introduced in (17).

For the calculation of phase diagrams by means of the minimization of the Gibbs energy of the systems [19], we need to translate the information of (47) and (48), based on the chemical potentials of the components, into the effects of chain connectivity as manifested in the integral interaction parameter g. This expression reads [27]:

$$g_{AB} = \frac{\alpha_{AB}}{(1 - \nu_{AB})\,(1 - \nu_{AB}\varphi_B)} - \zeta_{AB}\left(\frac{2a + b}{3} + \frac{b - a}{3}\varphi_B\right) \tag{49}$$

For the partial Gibbs energies [cf. (4)] of the component i one obtains:

$$\frac{\Delta\overline{\overline{G}}_i}{RTN_i} = \frac{1}{N_i}\ln\varphi_i + \left(\frac{1}{N_i} - \frac{1}{N_k}\right)\varphi_k + \chi_i\varphi_k^2 \tag{50}$$

where i and k are the components A and B. The composition dependencies of the differential interaction parameters, χ_i, can again be calculated from g (49) by analogy to (9) and (11).

Equation (49) formulated for blends of linear macromolecules also provides the facility to model blends of linear polymers (index L) and branched polymers (index B) synthesized from the same monomer [28]. If the end-group effects and dissimilarities of the bi- and trifunctional monomers can be neglected, the parameter α becomes zero. This means that the integral interaction parameter is determined by the parameter ζ_{LB}, i.e., the conformational relaxation, in combination with the intramolecular interaction parameters of the blend components. Because of the low values of Φ_A and Φ_B, the first terms in (47) and (48) can be neglected with respect to the second terms (for molar masses of the polymers that are not too low) so that one obtains the following expression:

$$g_{LB} = -\frac{\zeta_{LB}}{3}\left(\frac{2}{N_B\Phi_B} + \frac{1}{N_L\Phi_L} + \left(\frac{1}{N_L\Phi_L} - \frac{1}{N_B\Phi_B}\right)\varphi_B\right) \tag{51}$$

It is obvious that the conformational relaxation must be proportional to the degree of branching and approach zero upon the transition of the branched polymer to a linear polymer. For the sake of consistency and simplicity, we define the degree of branching, β, again in terms of intrinsic viscosities (cf. (27)) as:

$$\beta = 1 - \frac{\Phi_L^*}{\Phi_B} \tag{52}$$

where Φ_L^* is the volume fraction of segments in an isolated linear coil consisting of the same number of segments as the branched polymer under consideration. We can then write, expanding ζ_{LB} in a series with respect to β and maintaining only the first term for the following calculations, referring to moderately branched polymers:

$$\zeta_{LB} = Z\beta\left(+H\beta^2 + \cdots\right) \tag{53}$$

Under the premises formulated above and eliminating the different Φ values by means of (27) and (29) as before, the expression for g becomes:

$$g_{LB} = -\kappa Z\beta\left(\frac{1+\varphi_B}{\sqrt{N_L}} + \frac{2-\varphi_B}{\sqrt{N_B}} - \frac{\beta(2-\varphi_B)}{\sqrt{N_B}}\right) \tag{54}$$

where κ is a constant, which can be calculated from the parameter $K_{L,\Theta}$ of the Kuhn–Mark–Houwink relation (29) of the linear polymer for theta conditions and the density of this polymer as:

$$\kappa = \frac{K_{\mathrm{L},\Theta}\,\rho_{\mathrm{L}}}{3} \tag{55}$$

The only information required for model calculations concerning the incompatibility of linear and branched polymers on the basis of (54) concerns β, the degree of branching of the nonlinear component, κ (i.e., the viscosity–molecular weight relationship for the linear polymer under theta conditions) and the polymer density, plus $\mathrm{Z} = \zeta_{\mathrm{AB}}/\beta$, the conformational response of the system normalized to β [cf. (53)].

2.1.3 Mixed Solvents

For the modeling of ternary systems(the topic of the next section), the applicability of (26) to mixtures of low molecular weight liquids would be very helpful, because of the possibility to describe all subsystems by means of the same relation. First experiments [29], presented in Sect. 4, show that this is indeed possible. This means that (26) remains physically meaningful upon the reduction of the number of segments down to values that are typical for low molecular weight compounds. With respect to λ one must, however, keep in mind that this parameter loses its original molecular meaning.

2.2 Ternary Systems

The segment molar Gibbs energy of mixing for three component (indices i, j, and k) with N_i, N_j, and N_k segments, respectively, as formulated on the basis of the Flory–Huggins theory reads in its general form:

$$\frac{\Delta\overline{\overline{G}}}{RT} = \frac{\varphi_i}{N_i}\ln\varphi_i + \frac{\varphi_j}{N_j}\ln\varphi_j + \frac{\varphi_k}{N_k}\ln\varphi_k + g_{ij}\varphi_i\varphi_j + g_{ik}\varphi_i\varphi_k + g_{jk}\varphi_j\varphi_k + t_{ijk}\,\varphi_i\,\varphi_j\,\varphi_k \tag{56}$$

The first three terms stand for the combinatorial part of the Gibbs energy, the next three terms represent the residual contributions stemming from binary interactions, and the last term accounts for ternary contacts.

The double-indexed g parameters are for binary interaction parameters. The first line of the above relation represents the combinatorial part, and the second line the residual part of the reduced segment molar Gibbs energy of mixing. This relation also contains a ternary interaction parameter t_{ijk} that accounts for the expectation that the interaction between two components of the ternary mixture may change in the presence of a third component.

Because of the well-documented composition dependencies of the individual binary interaction parameters, an unmindful use of (56) would lead to totally unrealistic results. This feature requires twofold adaption.

First of all, it is necessary to account for the fact that the contribution of a certain binary contact to the total Gibbs energy of mixing depends on its particular molecular environment, which in the general case also contains the third component. We can allow for that circumstance by multiplying g_{ij} with the factor $(\varphi_j + \varphi_i) = (1 - \varphi_k) \leq 1$.

Secondly, we need to specify whether the composition dependencies of the g_{ij} parameters are formulated in terms of φ_i or of φ_j, because the resulting mathematical expressions are not identical.

In order to enable a straightforward application of the new approach to the most interesting ternary systems (polymer solutions in mixed solvents and solutions of a polymer blend in a common solvent), it is expedient to express the binary interaction parameters for polymer solvent systems (26) and that for polymer blends (49) in the same form. This requirement is met by the relation:

$$g_{ij} = \frac{\alpha_{ij}}{\left(1 - v_{ij}\right)\left(1 - v_{ij}\varphi_j\right)} - \zeta_{ij}\left(\delta_{ij} + \varepsilon_{ij}\,\varphi_j\right) \tag{57}$$

For polymer solutions:

$$\delta = 1 \quad \text{and} \quad \varepsilon = (1 - \lambda) \tag{58}$$

whereas the corresponding equation for a polymer blend (the composition dependence being expressed in terms of φ_B) reads:

$$\delta = \frac{2a + b}{3} \quad \text{and} \quad \varepsilon = \frac{b - a}{3} \tag{59}$$

By means of (57) and the required modification formulated at the beginning of this section, one obtains the following expression for the reduced residual segment molar Gibbs energy of mixing of ternary systems, if one neglects ternary interactions ($t_{ijk} = 0$) for the time being:

$$\begin{aligned}\frac{\Delta\overline{\overline{G}}^{\,\mathrm{res}}}{RT} = &\left[\frac{\alpha_{12}}{(1 - v_{12})(1 - v_{12}\varphi_2(1 - \varphi_3))} - \zeta_{12}(\delta_{12} + \varepsilon_{12}\,\varphi_2(1 - \varphi_3))\right]\varphi_1\varphi_2 \\ &+ \left[\frac{\alpha_{23}}{(1 - v_{23})(1 - v_{23}\varphi_3(1 - \varphi_1))} - \zeta_{23}(\delta_{23} + \varepsilon_{23}\,\varphi_3(1 - \varphi_1))\right]\varphi_2\varphi_3 \\ &+ \left[\frac{\alpha_{31}}{(1 - v_{31})(1 - v_{31}\varphi_1(1 - \varphi_2))} - \zeta_{31}(\delta_{31} + \varepsilon_{31}\,\varphi_1(1 - \varphi_2))\right]\varphi_3\varphi_1\end{aligned} \tag{60}$$

As one of the three composition variables becomes zero, this relation simplifies to the expression for binary mixtures (57). The extension of (60) to multicomponent systems is unproblematic and enables the calculation of phase diagrams for such mixtures of great practical importance if one calculates the composition of the coexisting phases by a direct minimization of the Gibbs energy [19]. In this manner, it is possible to evade the laborious and sometimes even impossible calculation of the chemical potential for each component.

The implementation of ternary interactions by simply adding the last term of (56) to (60) does not suffice. The reason lies in the fact that the three options to form a contact between all three components out of binary contacts (1/2 + 3, 1/3 + 2, and 2/3 + 1) might differ in their contribution to the Gibbs energy of the mixture. This supposition results in the necessity to introduce three different ternary interaction parameters. Furthermore, it requires a weighting of these contribution to account for the fact that they must be largest in the limit of the first addition of the third component 3 (highest fraction of 1/2 contacts) and die out as component 3 becomes dominant (vanishing fraction of 1/2 contacts). The simplest possibility to account for $\Delta\overline{\overline{G}}_{\mathrm{t}}^{\mathrm{res}}$, the extra contributions of ternary contacts to the residual Gibbs energy, is formulated in (61), where the negative sign was chosen by analogy to the second term of (57):

$$\frac{\Delta\overline{\overline{G}}_{\mathrm{t}}^{\mathrm{res}}}{RT} = -[t_1(1-\varphi_1) + t_2(1-\varphi_2) + t_3(1-\varphi_3)]\varphi_1\,\varphi_2\,\varphi_3 \tag{61}$$

t_1 quantifies the changes associated with the formation of a ternary contact 1/2/3 out of a binary contact 2/3 by adding a segment of component 1. The meaning of t_2 and t_3 is analogous.

Equation (61) makes allowance for differences in the genesis of ternary contacts but it does not yet consider that the number of segments of the third component in the coordination sphere of a certain binary contact might deviate from that expected from the average composition due to very favorable or unfavorable interactions (quasi chemical equilibria). One way to model such effects consists of the introduction of composition-dependent ternary interaction parameters, as formulated in the following equation:

$$\begin{aligned}\frac{\Delta\overline{\overline{G}}_{\mathrm{t}(\varphi)}^{\mathrm{res}}}{RT} = &-[(t_1 + t_{11}\varphi_1)(1-\varphi_1) + (t_2 + t_{22}\varphi_2)(1-\varphi_2) \\ &+ (t_3 + t_{33}\varphi_3)(1-\varphi_3)]\varphi_1\varphi_2\varphi_3\end{aligned} \tag{62}$$

The relations presented for ternary mixtures open the possibility for investigation of the extent to which their thermodynamic behavior can be forecast (neglecting possible contributions of ternary interaction parameters) if the binary interaction parameters of the three subsystems are known as a function of composition from independent experiments. For such calculations, it is important to make sure that the size of a segment is identical for all subsystems. The fact that most of the

experimental information available for polymer solutions uses the molar volume of the particular solvent to fix the size of a segment, requires a conversion in the case of polymer solutions in mixed solvents. If one chooses the molar volume of solvent 1 to define the common segment, this means that the binary interaction parameter for the solvent 2 must be divided by the ratio of the molar volumes $\overline{V}_1/\overline{V}_2$.

3 Measuring Methods

Experimental information concerning the thermodynamic properties of mixtures is primarily accessible via phase equilibria [30]. In the case of polymer solutions, vapor pressure measurements (liquid/gas equilibria) constitute the most important source of data because of the nonvolatility of the solutes and because of the comparatively large composition interval (typically ranging from some 25% to almost pure polymer) over which this method yields reliable data. In order to obtain a complete picture from infinitely dilute solutions up to almost pure polymer melt, these data need to be complemented by further methods. Osmometry (liquid/liquid equilibria) provides χ_o, the Flory–Huggins interaction parameter in the limit of pair interaction between the polymer molecules; this information is also accessible via scattering methods (light or neutrons), which monitor the composition dependences of the chemical potentials. Most published data refer to dilute and moderately concentrated solutions. It is difficult to study the range of vanishing solvent concentration because of the high viscosity of such mixtures. Inverse gas chromatography (IGC) is one of the few sources of information. Thermodynamic information for polymer blends is usually based on small angle neutron scattering. The following sections (Sects. 3.1–3.3) outline how the different methods work and cite some recent relevant publications in this area.

3.1 Vapor Pressure Measurements

The classical method consists of the quantitative removal of air from polymer solutions coexisting with a gas phase and measurement of the equilibrium pressures of the solvent above the solution by means of different devices. Such experiments are very time consuming because the liquid mixtures must be frozen-in and the air that accumulates in the gas phase must be pumped off. In order to obtain reliable data this procedure must be repeated several times to get rid of all gases. By means of this approach it is practically impossible to accumulate comprehensive information for a large number of systems.

For the reasons outlined above, alternative methods were developed that avoid the measurement of absolute vapor pressures. One procedure combines head space sampling with conventional gas chromatography (HS–GC) [31] and yields relative vapor pressures, normalized to the vapor pressure of the pure solvent. A well-defined volume of the equilibrium gas phase is taken out from a thermostated vial

sealed with a septum by means of a syringe and transferred to a gas chromatograph. The amount of the solvent is registered either in a flame ionization detector (FID) or by means of a cell measuring the thermal conductivity of the gas stream. Such measurements yield the ratio p/p_o, which in many cases can be taken as the activity of the solvent. Whether corrections for the nonideality of the gas are required or not must be checked in each case. The main work required with this method consists of the optimization of the HS–GC, i.e., determination of the best operation procedures for gas sampling, gas chromatography, and data evaluation. However, once these parameters have been determined, HS–GC offers quick access to thermodynamic data because the method is automated.

Another possibility for avoiding the measurement of absolute vapor pressures is provided by sorption methods. In most cases, the polymer is positioned on a quartz balance and the amount of solvent it takes up via the vapor phase is weighted. The so-called "flow-through" variant [32] works with an open system in contrast to the previous method.

Isopiestic [33] experiments also offer access to chemical potentials. This method monitors the conditions under which the vapor pressures above different solutions of nonvolatile solutes (like polymers or salts) in the same solvent become identical, where one of these solutions is a standard for which the thermodynamic data are known. These experiments can be considered to be a special form of differential osmometry (cf. Sect. 3.2) where the semi-permeable membrane, separating two solutions of different composition, consists of the gas phase.

3.2 Osmometry and Scattering Methods

Measurements performed to determine the molar masses of polymers yield – as a valuable byproduct – information on the pair interaction between the macromolecules [30]. The composition dependence of the osmotic pressure π_{osm} observed via membrane osmometry is directly related to the chemical potential of the solvent [cf. (14) of Sect. 2] and provides the second osmotic virial coefficient A_2, from which χ_o, the Flory–Huggins interaction parameter in the limit of high dilution becomes accessible [cf. (15)]. Such data are particularly valuable because they can be measured with higher accuracy than the χ values for concentrated polymer solutions and because they represent a solid starting point for the sometimes very complex function $\chi(\varphi)$. In principle, membrane osmometry can also be operated with polymer solutions of different composition in the two chambers (differential osmometry) to gain data for higher polymer concentrations; however, little use is made of this option.

Scattering methods represent another route to A_2 and χ_o; these experiments do not monitor the chemical potential itself but its composition dependence. Light scattering – like osmosis – can in principle also yield information for polymer solutions beyond the range of pair interaction, but corresponding reports are seldom. In contrast, small

angle neutron scattering is an important source of thermodynamic information for polymer blends over the entire composition range.

3.3 Other Methods

In addition to the experiments briefly discussed above, two further equilibrium methods and two nonequilibrium procedures are sometimes employed to obtain thermodynamic information.

The most frequently used additional method is the evaluation of data for liquid/liquid phase separation, i.e., of critical points and of binodal curves [21]. This information is normally obtained by means of cloud point measurements (either visually or turbidimetrically) and the analysis of the composition of coexisting phases. Critical data give access to the system-specific parameters via the critical conditions, as formulated in (36) and (37) for the present approach or by means of equivalent expressions of other theories. If the critical data (temperature, pressure, and composition) are known for a sufficiently large number of polymer samples with different molar mass, and the number of parameters required for a quantitative description of $g(\varphi)$ is not too high, this method yields reliable information. Similar consideration also hold true for the evaluation of binodal curves. In both cases it is very helpful to formulate a theoretically justified temperature dependence of the system-specific parameters.

Liquid/solid equilibria also offer access to thermodynamic information. In this case, it is the differential interaction parameter ξ of the *polymer* that is obtained according to (38) from the known molar mass of the polymer, its melting temperature in the pure state, and the corresponding heat of melting plus the polymer concentration in the solution that is in equilibrium with the pure polymer crystals. Because of the well-known problems in obtaining perfect crystals in the case of macromolecules, special care must be taken with the evaluation of such data.

Vapor pressure osmometry [34–36] constitutes a very helpful nonequilibrium method for obtaining thermodynamic information for solutions of oligomers and polymers of low molar mass, for which osmometry and light scattering experiments do no longer yield reliable data. Such experiments are based on the establishment of stationary states for the transport of solvent via the gas phase from a drop of pure solvent fixed on one thermistor to the drop of oligomer solution positioned on another thermistor. Because of the heats of vaporization and of condensation, respectively, this transport process causes a time-independent temperature difference from which the required information is available after calibrating the equipment.

Inverse gas chromatography (IGC) represents another nonequilibrium method; it yields valuable information on polymer–solvent interactions in the limit of vanishing solvent content [37, 38]. In experiments of this type, a plug of solvent vapor is transported in a column over a stationary phase consisting of the pure polymer melt. The more favorable the solvent interaction with the polymer, the longer it takes

until the plug leaves the column. An adequate evaluation of the observed retention times yields access to the chemical potentials of the solvent, i.e., to Flory–Huggins interaction parameters in the limit of $\varphi \rightarrow 1$.

4 Experimental Results and Modeling

4.1 Binary Systems

4.1.1 Polymer Solutions

Organic Solvents/Linear Homopolymers

This section gives examples for the typical thermodynamic behavior of polymer solutions. The first part deals with homogeneous mixtures and discusses the molecular weight dependence of second osmotic virial coefficients, the role of glass transition for the determination of interaction parameters, and the reasons for changes in the sign of the heat of dilution with polymer concentration. The second part of this section is dedicated to liquid/liquid phase separation and – among other things – explains in terms of the present approach, why 1,2-polybutadiene is completely miscible with *n*-butane but 1,4-polybutadiene is not.

One of the major consequences of the thermodynamic approach used here is the postulate that the second osmotic virial coefficients may increase with rising molar mass of the polymer, even for good solvents (better than theta conditions), in contrast to the statements of current theories. Figure 2 shows an example of this behavior, which was already observed by Flory and coworkers [22] in the 1950s and confirmed by independent measurements [39].

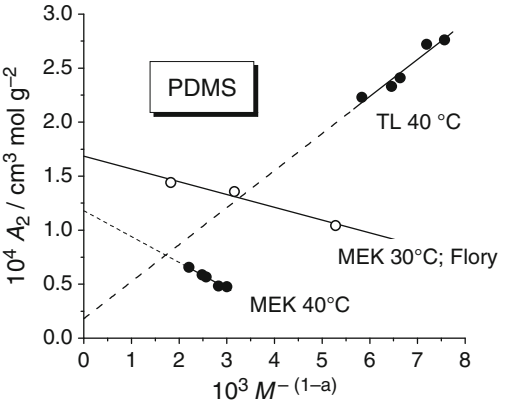

Fig. 2 Molecular weight dependence of the second osmotic virial coefficient for the systems [22, 39] methyl ethyl ketone (MEK)/PDMS and TL/PDMS represented according to (31)

As postulated by (31), the molecular weight dependence of A_2 should not be represented in double logarithmic plots, but as a function of $M^{-(1-a)}$, where a is the exponent of the Kuhn–Mark–Houwink relation. In contrast to the customary evaluation (in double logarithmic plots), this procedure does not in the general case lead to zero A_2^{∞} values; in most cases they are very small but, outside experimental errors, different from zero.

The following example of the composition dependence of the Flory–Huggins interaction parameter pertains to the system cyclohexane/poly(vinyl methyl ether) (CH/PVME) [23]. Except for χ_o, obtained via osmometry, all data stem from vapor pressure measurements [40]. This system does not fit into the normal scheme because CH is a good solvent for PVME, despite uncommonly large χ_o values of the order of 0.5. For good solvents, χ_o is usually considerable less than 0.5; for theta solvents, χ_o is typically equal to 0.5 and it increases upon the approach of phase separation. The curves combining the data points in Fig. 3 were calculated by adjusting the parameters of (32). Within the scope of the present approach, the high solvent quality results from fact that the χ values decrease considerably as φ increases so that they are favorable within the range of moderate polymer concentrations, where the system becomes very susceptible to phase separation.

The minima of $\chi(\varphi)$ shown in Fig. 3 represent a consequence of the dissimilar contributions of the dilution in two steps, as demonstrated in Fig. 4. The first term, quantifying the effects of contact formation, is Gibbs energetically very unfavorable and increases with rising polymer concentration because of the parameter v. By contrast, the second term, standing for the contributions of the conformational relaxation, is highly favorable and the more so, the larger φ becomes. The observed minimum in $\chi(\varphi)$ is caused by the fact that the first summand increases more than linearly, whereas the second decreases linearly.

Figure 4 also documents the general observation that the contributions of the two terms of (32) to the measured functions $\chi(\varphi)$ are markedly larger than χ itself; this situation is very similar to the build up of the Gibbs energy from enthalpy and entropy contributions. However, it is not permissible to interpret these terms in this

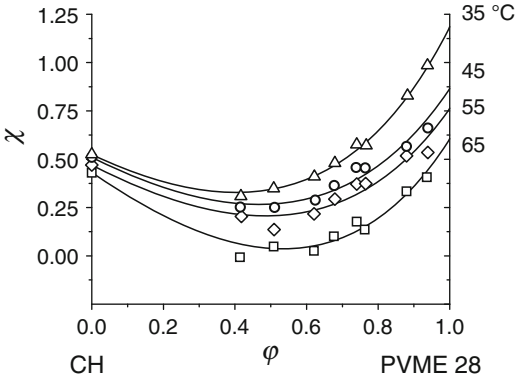

Fig. 3 Composition dependence of Flory–Huggins interaction parameter for the CH/PVME system at the indicated temperatures [40]; the curves are calculated according to (32). *PVME 28* indicates that the M_w of the PVME is 28 kg/mol

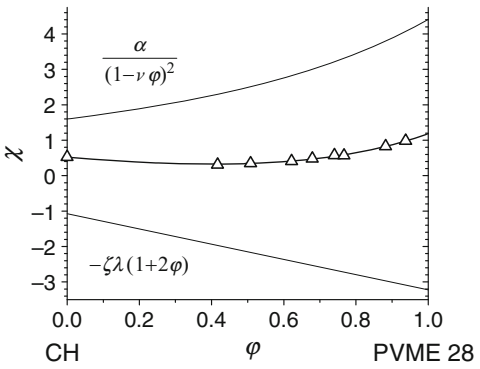

Fig. 4 Breakdown of the composition dependence of χ into the contributions resulting from the two steps of dilution (cf. Fig. 1 and (32), $\alpha = 1.599$, $\nu = 0.398$, and $\zeta\lambda = 1.074$) for the CH/PVME 28 system at 35°C

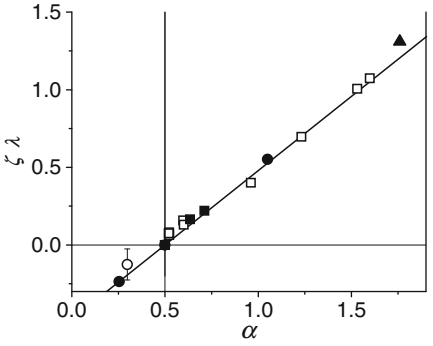

Fig. 5 Interrelation between the leading parameters of (32). *Closed symbols* data from A_2 (M) [39]; *open symbols* data from $\chi(\varphi)$ [23]. Each symbol stands for a different polymer/solvent system, the polymers being PS, PMMA, polyisobutylene, and PDMS

manner: Both terms can be split into their enthalpy and entropy parts, as will be shown later.

Another point of view on the contributions of the two terms of (32) deserves special attention. Namely, the expectation according to the present approach that their leading parameters, α and ζ, should not be independent of each other. The reason for this surmise lies in the fact that contact formation and conformational relaxation share the same thermodynamic background, i.e., the effects of the conformational relaxation of the components should strongly correlate with the effects of contact formation, as discussed in Sect. 2.

The results shown in Fig. 5 demonstrate that there indeed exists such a general interrelation, where each data point represents a certain system and temperature. The results of this graph demonstrate the consistency of the approach because the data [39] obtained from the evaluation of the molecular weight dependence of A_2 (cf. Fig. 2) and from the composition dependence of $\chi(\varphi)$ (an example [40] is shown in Fig. 3) lie on the same line [here $\zeta\lambda = (0.957 \pm 0.00027) \times (\alpha - 0.5)$], despite the fundamentally different experimental methods used for their determination. For the common representation of the data, the ζ values reported in table 2 of [39] were multiplied by -0.5 (i.e., λ was set at 0.5), which is permissible for sufficiently large

molar masses of the polymer. The negative sign of this factor results from the fact that ζ of [39], used for the evaluation of A_2(M), was defined with the opposite sign of ζ as compared with the modeling of $\chi(\varphi)$. The reason lies in the interrelation between χ_o and A_2 formulated in (15).

It appears interesting that the interrelation between the leading parameters of the present approach shown in Fig. 5 for simple systems, i.e., for absence of special interactions between the components, is generally valid and holds true for all hitherto studied polymer solutions.

The modeling of homogeneous systems has so far been exemplified by means of solutions of polymers that are liquid at the temperatures of interest. Such systems are, however, the exception rather than the rule, because of the comparatively high glass transition temperatures of most polymers. Typical polymer solutions solidify upon a sufficient augmentation of polymer concentration and the question arises of how this feature is reflected in the thermodynamic data. To study the importance of this loss in the mobility of the polymer chains for the determination of Flory–Huggins interaction parameters, we have studied solutions of PS in different solvents [41] within the temperature range of 10–70°C. These experiments demonstrate that the consequences of the freezing-in of the polymer motion at high polymer concentrations for the measured vapor pressures depend on the thermodynamic quality of the solvent and on the experimental method employed for the measurement.

Figure 6 shows the reduction of the vapor pressures of toluene (TL, a good solvent) and of CH (a marginal solvent) as the concentration of PS rises. As long as the mixtures are liquid these curves display the interaction in the usual manner, i.e., the reduced vapor pressure of TL is considerable lower than that of CH because of the more favorable interaction with the polymer. In the case of CH, this dependence continues smoothly into the glassy range, whereas a discontinuity is observed for TL.

Based on the results shown in Fig. 6, one is tempted to postulate that the solvent quality loses its importance once the solutions become glassy. However, the situation is more complicated under nonequilibrium conditions, as discussed by means of Fig. 7. This graph contains two types of experimental data, one set obtained via

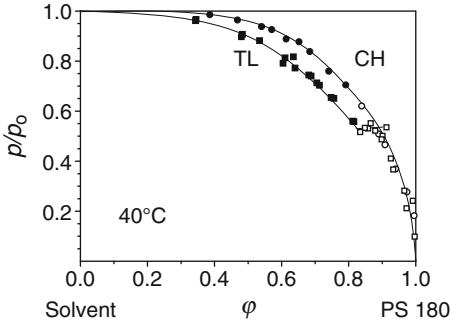

Fig. 6 Dependencies of the reduced vapor pressures of TL (*squares*) and of CH (*circles*) on the volume fraction of PS at 40°C [41]. *Closed symbols* liquid mixtures, *open symbols* glassy mixtures

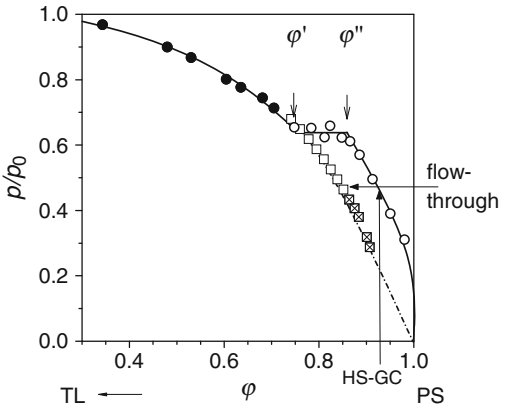

Fig. 7 Reduced vapor pressure of TL as a function of the volume fraction of PS measured at 20°C with either HS–GC (*closed circles* liquid solutions, *open circles* glassy mixtures), or at 30°C, by means of the flow-through method [32] (*squares*). According to [32], the *crossed squares* refer to compositions inside the range of glassy solidification; no information is given for the *open squares*. *Lines* are guides for the eye

HS–GC as usual and another set [32] obtained by means of the so-called "flow through" method, which differs fundamentally.

The vapor pressure data obtained by means of HS–GC measurements for the solutions of PS (below the glass transition temperature of the polymer) in the favorable solvent TL resemble closely the results for the solutions of polyethylene oxide (PEO) in chloroform (below the melting temperature of the polymer), as shown later. The common denominator of these processes lies in the loss of mobility of the macromolecules. The results presented in Fig. 7 can be interpreted in the following manner: The composition range of constant vapor pressure ($\varphi' \leq \varphi \leq \varphi''$) observed with HS–GC measurements reflects the coexistence of two kinds of microphases, one in which the polymer mobility is identical with that in the liquid state at the composition φ', and a glassy microphase of composition φ'', where the segmental mobility is fully frozen-in. The reason why this sort of "tie line" can be observed with HS–GC but not with flow-through experiments lies in the fact that the former method uses a closed system, in contrast to the latter in which additional vapor is always available. Because it is the vapor pressure that is constant in flow-through experiments and not the composition of the mixture, the amount of solvent taken up by the polymer can be constantly replaced. This process comes to an end either as the equilibrium vapor pressure of the liquid mixture is reached at the composition φ' or as kinetic impediments become too large. The two methods under consideration complement each other: HS–GC monitors the upper limit φ'' of the solidification interval, whereas the flow-through method displays its lower limit φ'. Concerning the evaluation of vapor pressures measured via HS–GC above solidified polymer solutions, it is obvious from the present results that such information must not be used to establish $\chi(\varphi)$ dependencies, particularly in the case of thermodynamically favorable solvents.

To conclude the treatment of homogenous solutions of polymers in organic solvents, we deal with the temperature dependencies of the parameters of (32). The knowledge of these changes enables their separation in enthalpy and entropy

contributions as formulated in (39) and (40) for χ. In this context, it is of particular interest to check whether the approach helps the rationalization of observed changes in the sign of the heat of dilution upon a variation of the polymer concentration. Solutions of PS in *tert*-butyl acetate (TBA) were chosen for this purpose because of the large temperature interval that was studied for this system. The combination of three different methods was used to obtain interaction parameters in all composition regions of interest: (1) light scattering measurements for dilute solutions in closed cells [42], (2) the determination of absolute vapor pressures (not HS–GC, quantitative removal of air) up to temperatures well above the boiling point of the pure solvent [43], and (3) IGC [37] close to the polymer melt.

The analysis [44] of the thus-obtained temperature dependencies of the system-specific parameters of (32) with respect to the individual enthalpy contributions of the two steps of dilution (cf. Fig. 1), yields $\chi_{H,fc}$ and $\chi_{H,cr}$. How these heat effects depend on polymer concentration is shown for the system TBA/PS at 110°C in Fig. 8.

This graph makes it immediately obvious that the insertion of a solvent molecule between contacting segments at constant conformation of the components constitutes an exothermal process ($\chi_{H,fc} < 0$) at high dilution, whereas the conformational relaxation is endothermal ($\chi_{H,cr} > 0$). In both cases, the absolute values of the heat effects increase with rising polymer concentration. However, the slopes of these two dependencies differ in such a manner that the total heat of dilution is exothermal for low φ values, but endothermal for high polymer concentrations. With the present example, this finding can be rationalized qualitatively in terms of the composition dependence of free volumes and excess volumes. The pure solvent is already highly expanded and the polymer molecules may fill some of the existing voids (this should lead to negative excess volumes and to the evolution of heat, due to the formation of new molecular interfaces). The pure melt, on the other hand, is still densely packed at the same temperature and the addition of a solvent molecule might cause an expansion in volume (resulting in positive excess volumes and in the consumption of heat).

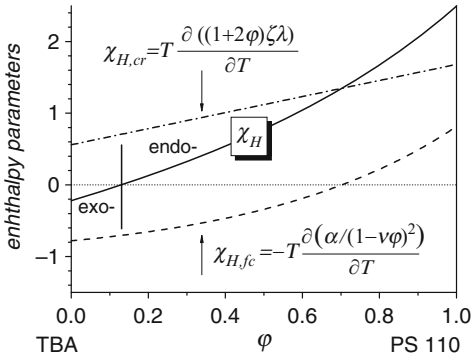

Fig. 8 Composition dependence of the enthalpy part of the Flory–Huggins interaction parameter χ for the system TBA/PS (M_w = 110 kg/mol, narrow molecular weight distribution) at 110°C as compared with the corresponding enthalpy contributions of the two steps of dilution [cf. Fig. 1 and (32)]. The experimental data were taken from [43]

There exist other examples for inversions in the heats of dilution; in these cases an analogous straightforward molecular interpretation appears difficult. For instance, the system TL/PS shows an inversion [44] from endothermal in the range of moderate polymer concentrations to exothermal at high φ values at 37°C. In this case, the sign of the heat contributions of the two steps of dilution are the same as in the previous case. However, here it is only $\chi_{H,cr}$ which increases (linearly) with rising polymer concentration, whereas $\chi_{H,fc}$ decreases (more than linearly). This combination of the two contributions leads to the opposite inversion, namely from endothermal to exothermal upon an augmentation of φ. Concerning the molecular reasons for this behavior, one may speculate on the basis of the present findings that the insertion of a TL molecule between two contacting PS segments (belonging to different molecules) becomes energetically particularly favorable in the limit of high polymer concentration.

So far, we have dealt exclusively with homogeneous systems; the following considerations concern the possibilities of obtaining the parameters of the present expression for $\chi(\varphi, T)$ from demixing data. The results will demonstrate that the present approach is capable of modeling liquid/liquid equilibria and liquid/gas equilibria with the same set of parameters, in contrast to traditional theories.

The first example refers to solutions of PS in CH. This is probably the system for which the phase separation phenomena are studied in greatest detail [45], namely in the temperature range from ca. 10 to 240°C and for molar masses from 37 to 2700 kg/mol. Figure 9 displays the experimental data [45] together with the modeling, using (32) to describe the Flory–Huggins interaction parameter as a function of composition.

The system-specific parameters used for the modeling of the phase diagrams were calculated from the critical data (T_c and φ_c) measured [45] for PS samples of different molar mass. For this purpose, the critical conditions resulting for the present approach [cf. (36) and (37)] were first simplified: The parameter λ was set at 0.5 (this does not imply a loss of accuracy for the system of interest) and the interrelation between α and $\zeta\lambda$ [cf. (34)] was used to eliminate the parameter α; setting $E = 0.847$ (an average value for solutions of vinyl polymers in organic solvents). This procedure reduces the number of parameters from four to only two (ζ and v) and enables the calculation of their values from the critical temperature by inserting the known numbers of segments N and the critical composition φ_c in the two critical conditions and solving these equations. Because of the large number of different molar masses, yielding different critical data, it is possible to model the temperature dependencies of the parameters ζ and v. The observed maximum in $\zeta(T)$ is expected because of the transition from an upper critical solution temperature (UCST) behavior at low temperatures to a lower critical solution temperature (LCST) behavior at high temperatures, in combination with the fact that $\zeta = 0$ at the theta temperature, irrespective of the sign of the heat of mixing; $v(T)$ also passes a maximum but at a much lower temperature (in the vicinity of the endothermal theta temperature). Within the range of LCSTs, both parameters decrease with rising temperature. The binodal and spinodal curves shown in Fig. 9 for the different PS samples were calculated from the thus-obtained system-specific parameters using

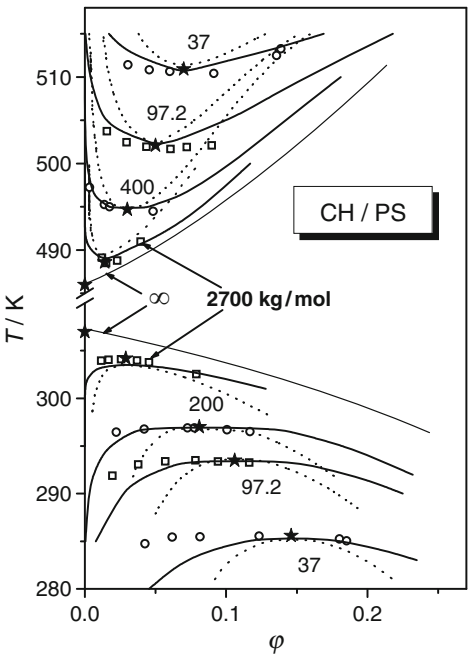

Fig. 9 Phase diagram (demixing into two liquid phases) of the system CH/PS for the indicated molar masses of the polymer (kg/mol). Cloud points (*open symbols*) and critical points (*stars*) are taken from the literature [45]. The data for the high temperatures refer to the equilibrium vapor pressure of the solvent. Binodals (*solid lines*) and spinodals (*dotted lines*) were calculated as described in the text by means of the temperature-dependent parameters [46] ζ and v

the method of the direct minimization of the Gibbs energy [19], instead of equality of the chemical potentials of the components as the equilibrium condition.

The agreement of information concerning the composition dependence of the Flory–Huggins interaction parameter obtained from different sources is demonstrated by means of Fig. 10. The data points display the results of vapor pressure measurements and the dashed line stems from the evaluation of critical demixing data described above. The interaction parameter is calculated according to (6), (5), and (32) by reading the ζ and v values from figure 2 of [46] for 308 K, setting $\lambda = 0.5$ and $E = 0.847$. To the author's knowledge, this is the first time that liquid/gas and liquid/liquid phase equilibria have been modeled accurately by the same set of parameters, where only two were adjusted to the experimental data in the present case.

For some technical processes and polymer applications, pressure represents an important variable. For this reason, the extent to which the present approach is suited to describe pressure effects was checked. By means of demixing data as a function of pressure published for the system *trans*-decalin/PS [49] it was shown [46] that (32) is also apt for that purpose.

The systems *n*-butane/1,4-polybutadiene (98% cis) [*n*-C_4/1,4-PB] and *n*-butane/1,2-polybutadiene [*n*-C_4/1,2-PB] are the next examples for the modeling of Flory–Huggins interaction parameters [50]. In this case, it appeared particularly interesting to understand why 1,2-PB is totally miscible with *n*- C_4 but 1,4-PB is not. In these experiments we measured the absolute vapor pressures (i.e., not using

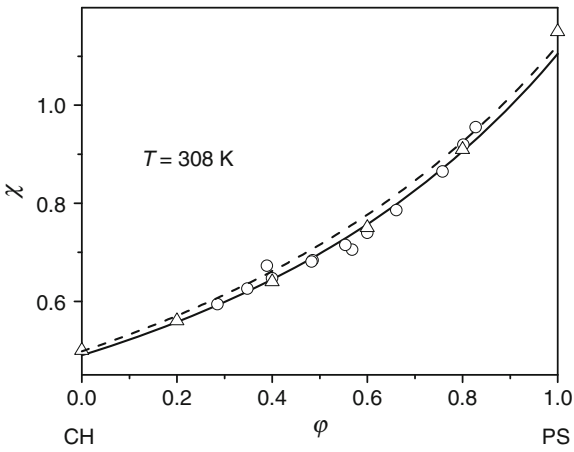

Fig. 10 Comparison of the composition dependence of the Flory–Huggins interaction parameter determined for the CH/PS system at 308 K either from liquid/gas equilibria (*triangles* [47] and *circles* [48]), jointly represented by the solid line, or from liquid/liquid equilibria [46] (*dashed line*)

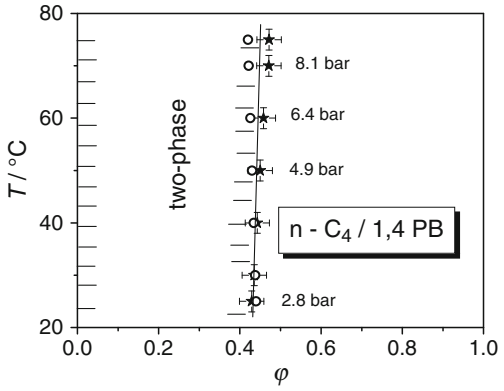

Fig. 11 Isochoric phase diagram for the system *n*-C_4/1,4-PB [50]. The measured data points are drawn as *stars* and those calculated by means of the interaction parameters obtained from the vapor pressure measurements as *circles*

HS–GC) because of the high volatility of *n*- C_4, and studied the segregation of a second liquid phase for the solutions of 1,4-PB under isochoric conditions (instead of the usual isobaric procedure). Figure 11 shows the thus-obtained phase diagram together with the miscibility gap calculated from the measured vapor pressures. Here, it is worth mentioning that the Sanchez–Lacombe theory [4, 51] models the vapor/liquid equilibria for the present systems very well but fails totally when the parameters obtained from such measurements are applied for the calculation of liquid/liquid equilibria.

The good agreement between the prediction of the miscibility gap from liquid/gas equilibria with the actual behavior is a further example of the utility of this approach. The extension of the Flory–Huggins theory by incorporating further contributions of chain connectivity and accounting for the phenomenon of

conformational relaxation also enables the rationalization of the fundamentally different solubilities of 1,4-PB and 1,2-PB. The 1,2-isomer interacts favorably with n-C_4 because the flexibility of the polymer backbone (pending double bonds) enables the establishment of suitable contacts with the surrounding solvent molecules. With the 1,4-isomer, on the other hand, such a rearrangement is largely impeded because the double bonds are now located in the main chain and make the conformational response much more difficult.

All examples shown so far refer to solutions of noncrystalline polymers. We will now discuss the solutions of a crystalline polymer, namely PEO in chloroform. Figure 12 gives an example of the primary data that can be obtained by measuring the reduced vapor pressure of the solvent by means of HS–GC.

According to the present results, it is possible to distinguish three clearly separable composition ranges, I–III (see Fig. 12). Only for range III do the data not depend on the details of film preparation, i.e., yield equilibrium information. The situation prevailing in the other ranges is discussed in terms of the addition of $CHCl_3$ to solid PEO. Within range I ($1 > w > w''$), the vapor pressure increases steadily up to a characteristic limiting value located well below that of the pure solvent. Within range II ($w'' > w > w'$), p_1 remains constant, despite the addition of further solvent. Finally, within range III ($w' > w > 0$), the vapor pressure rises again and approaches the value of the pure solvent. Range I should be absent for fully crystalline polymers; its existence is due to the amorphous parts of PEO, which can take up solvent until w' is reached. Range II results from the coexistence of the saturated solution with variable amounts of polymer crystals. Finally, no solid material is available in range III and we are back to the normal situation encountered with the solutions of amorphous polymers. According to the present results, it is practically impossible to reach thermodynamic equilibria within range I. Vapor pressures and degrees of crystallinity depend markedly on the details of sample preparation. Measurements within range III do not present particular problems with

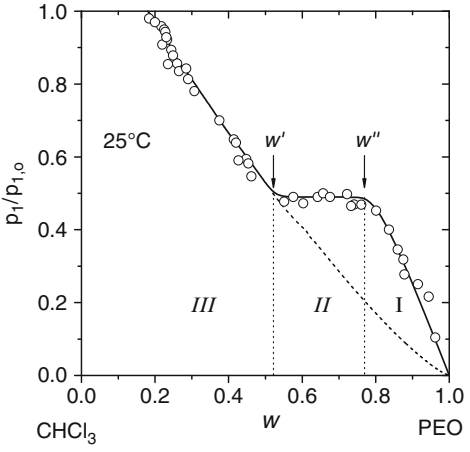

Fig. 12 Reduced vapor pressure of chloroform above solutions of PEO at 25°C as a function of the weight fraction w of the polymer [52]. The three composition ranges are labeled *I*, *II*, and *III*. The *dotted line* extrapolates the behavior of the homogeneous mixtures into the two-phase range

the attainment of equilibria. Range II assumes an intermediate position in this respect.

The observed nonequilibrium behavior at high polymer concentrations can be interpreted in terms of local and temporal equilibria, which are frozen-in during film preparation, i.e., in the course of solvent removal or quenching of the polymer melt. For discussion of these effects it is helpful to compare the fraction of the polymer that does not participate in the liquid/vapor equilibrium with the degree of crystallinity as obtained from DSC measurements. The general findings that the former is always larger than the latter, and that the differences decrease upon dilution, are tentatively interpreted as a trapping of amorphous PEO inside the crystalline material during sample preparation and its gradual release by the addition of solvent. This hypothesis is supported by micrographs showing the existence of such occlusions.

For systems of the present type it is possible to obtain equilibrium information from two sources: in the usual manner via the vapor pressures of the solvent above the solutions within range III (chemical potential of the solvent) and additionally from the saturation composition w' of the polymer (chemical potential of the polymer). The thermodynamic consistency of these data was documented [52] by predicting w' (liquid/solid equilibrium) from the information of liquid/gas equilibria. This match of thermodynamic information from different sources is a further argument for the suitability to the present approach for the modeling of polymer-containing mixtures.

Organic Solvents/Nonlinear Homopolymers

This section deals with the extent to which differences in the molecular architecture of the polymer affects its interaction with a given solvent. In particular, the comparison of linear and branched macromolecules is of interest. In order to obtain a clear-cut answer and for a straightforward theoretical discussion it is important to exclude special end-group effects (i.e., to keep the chemistry of the terminal group as similar as possible to that of the middle groups) and to apply the same criteria to the branching sites. The example [24] chosen refers to solutions of linear and branched polyisoprene (PI) in CH and fulfills the above criteria reasonably well. The number of branching points per molecule of the nonlinear product lies between six and seven. Figure 13 shows the composition dependence of the Flory–Huggins interaction parameter for the two types of systems obtained from HS–GC measurements and from vapor pressure osmometry.

Linear PI interacts with CH considerably more favorably than does the branched analog in the temperature range from 25 to 65°C according to these results, irrespective of polymer concentration. This finding agrees well with the expectation based on the present approach, which states that the first term of (32) (quantifying the first step of dilution, cf. Fig. 1) should only be affected marginally by a transition from a linear to a branched architecture of the polymer, in contrast to

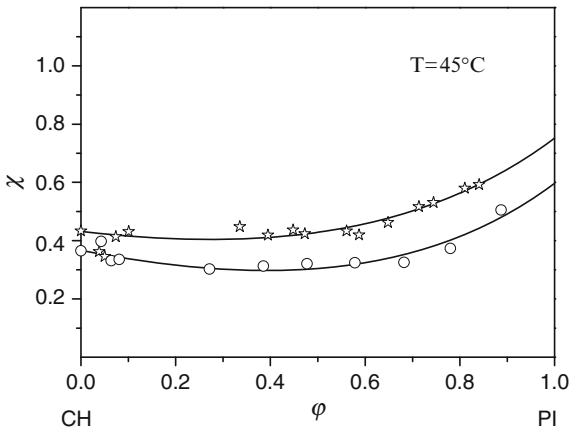

Fig. 13 Flory–Huggins interaction parameters for solutions of linear PI (*circles*, $M_w = 23.2$ kg/mol) and of branched PI (*stars*, $M_w = 21.6$ kg/mol) in CH as a function of polymer concentration

the second term (resulting from the conformational relaxation). This second summand is determined by the parameters λ and ζ, both of which depend on the molecular architecture of the polymer: A higher degree of branching leads to a reduction in the intramolecular interaction parameter λ (accumulation of the segments in a smaller volume) as well as in ζ (diminished possibilities to readjust to a changing molecular environment by conformational relaxation). Because of the negative sign of the second term, these changes lead to larger χ values for the branched polymer. In other words, in the absence of special effects, the thermodynamic quality of a given solvent declines upon an increase in the degree of branching. Another feature worth mentioning is the observation that the interrelation between the parameters $\zeta\lambda$ and α, established for linear macromolecules (cf. Fig. 5), remains valid for branched materials.

Organic Solvents/Linear Random Copolymers

With systems of this type, a new feature comes into play: In spite of the fact that we are dealing with binary systems, we need three different interaction parameters to describe the thermodynamic behavior. This makes the modeling considerably more difficult and is the reason why the present approach requires more adjustable parameters, and the theoretical understanding is far from being satisfactory.

For reasons outlined in the theoretical section (Sect. 2) (8) the study reported here uses weight fractions w instead of the usual volume fractions φ. It was carried out for solutions of poly(styrene-*ran*-methyl methacrylate [P(S-*ran*-MMA)], with different weight fractions f of styrene units, in $CHCl_3$, acetone (AC), methyl acetate (MeAc), and TL at 50°C [25]. Analogous measurement for the solutions of the corresponding homopolymers, PMMA and PS, were also performed for comparison.

For practical purposes, the possibility of predicting the thermodynamic behavior of random copolymers in a given solvent from knowledge of the corresponding homopolymers would be extremely helpful. The present results demonstrate that this is a difficult task and that the choice of the particular solvent plays a decisive role. For all systems under investigation, ${}_{\mathrm{w}}\chi$ varies considerably with the composition of the mixture. With one exception [$CHCl_3$/P(S-*ran*-MMA) and $f = 0.5$] the dependencies ${}_{\mathrm{w}}\chi(w)$ of the copolymers do not fall reasonably between the data obtained for the corresponding homopolymers. In most cases, the incorporation of a small fraction [25] of the monomer that interacts less favorably with a given solvent suffices to reduce the solvent quality for the copolymer, approximately to that for the worse soluble homopolymer. Figure 14 shows an example for which this effect is particularly obvious.

In terms of the ${}_{\mathrm{w}}\chi$ values measured for a given constant polymer concentration, the polar solvents $CHCl_3$, AC, and MeAc are expectedly more favorable for PMMA than for PS, whereas the nonpolar TL is a better solvent for PS than for PMMA. The shape of the functions ${}_{\mathrm{w}}\chi(w)$ varies considerably. For AC/PMMA and MeAc/PS, χ increases linearly and for AC/PS more than linearly, whereas it decreases linearly for $CHCl_3$/PS. With three of the systems, one observes minima in ${}_{\mathrm{w}}\chi(w)$, namely for TL/PMMA, TL/PS, and $CHCl_3$/PS; only MeAc/PMMA exhibits a maximum. On the basis of (32), this diversity of composition influences is easily comprehensible if one keeps in mind that the composition dependence of Flory–Huggins interaction parameters are made up of two separate contributions. The normally nonzero parameter ν of the first term of this relation (which is primarily determined by the differences in the shapes of monomeric units and solvents molecules) leads to a nonlinear composition dependence of ${}_{\mathrm{w}}\chi$, where the magnitude of this contribution increases as the absolute values of the parameter α rise. The second term of (32) adds a linear dependence, quantified by the parameter $\zeta\lambda$. In agreement with the great diversity of the systems concerning the functions ${}_{\mathrm{w}}\chi(w)$, all three parameters of the present approach may be positive, negative, or zero.

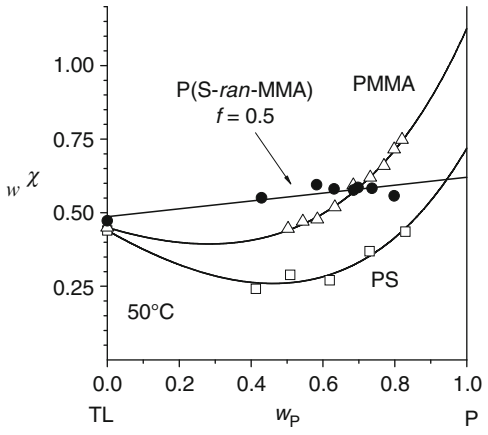

Fig. 14 Composition dependence of the Flory–Huggins interaction parameters [based on weight fractions w_P, cf. (8)] for the solutions of PS, PMMA, and of a random copolymer containing 50 wt% of these monomers in TL at 50°C [25]

The next aspect that deserves discussion concerns the quality of a given solvent for copolymers of different comonomer content, as compared with its quality for the corresponding homopolymers. The naive interpolation of the ${}_{w}\chi$ values for the copolymers between the data of the homopolymers according to their composition is at variance with the experimental observations. Only for the system $CHCl_3$/P(S-*ran*-MMA) with $f = 0.5$ does the composition dependence lie reasonably between the ${}_{w}\chi(w)$ curves for the homopolymers. All other solvents are approximately as poor for the copolymer ($f = 0.5$) as for the less favorably interacting homopolymer (PS in the case of AC and MeAc; PMMA in the case of TL). For the system TL/P(S-*ran*-MMA), studied in greater detail, the presence of only 10 wt% of styrene units suffice to raise ${}_{w}\chi$ to values that are within the range of high polymer concentration, even larger than that of the TL/PMMA system (see Figure 11 of [25]).

The dependencies of the system-specific parameters π on the weight fraction f of the styrene units in the copolymers can be well modeled by (41) for the different solvents. Linear functions, corresponding to $\pi^{E} = 0$, are exceptions and only observed for the parameters α and $\zeta\lambda$ with $CHCl_3$ and for ν with MeAc. For the polar solvents AC and MeAc, $\alpha(f)$ and $\zeta\lambda(f)$ exhibit maxima, whereas minima are observed for TL. The comparison of these excess parameters π^{E} obtained for the different solvents discloses another interesting feature, namely the fact that all excess parameters π^{E} exhibit the same sign for the three systems for which the behavior of the copolymer is dominated by the monomeric unit showing the less favorable interaction with the solvent. For α and $\zeta\lambda$, this means that an adverse excess contribution for contact formation is counteracted by a favorable conformational relaxation (AC and MeAc) or conversely, that a favorable excess contact formation goes along with an adverse conformational relaxation (TL).

In conclusion of this section, it is worthwhile noting that the interrelation of the system-specific parameters established for homopolymer solutions (cf. Fig. 5) also holds true for all copolymer solutions studied here (as demonstrated in Figure 15 of [25]).

Aqueous Solutions of Poly(vinyl methyl ether)

This example and the next (cellulose; Sect. 4.1.1.5) concern systems with uncommonly large α values (i.e., very unfavorable contact formation between the solvent and polymer segments) in combination with a similarly favorable conformational relaxation. Literature reports a very uncommon phase behavior [54, 55] for the system H_2O/PVME: The most striking feature is the occurrence of two minima in the cloud point curves instead of one. In addition to the normal critical point at low polymer concentration, the authors report a second critical point at high polymer concentrations for high molar masses of the polymer. Furthermore, they describe a three-phase line occurring at a certain characteristic temperature, even for strictly binary mixtures. The authors used a three-membered series expansion of the integral Flory–Huggins interaction parameter g with respect to φ for the modeling

[55] of their results and confined the temperature influences to the composition-independent term, assuming a linear dependence on $1/T$ to reproduce the observed phase separation upon heating.

The following considerations [53] deal with the question of which criteria (in terms of the system-specific parameters of the present approach) a certain system must fulfill to reproduce the anomalous phase separation phenomena reported in the literature. To that end, the condensed parameter $\zeta\lambda$ is eliminated from the critical conditions calculated on the basis of (33) to yield expressions analogous to (36) and (37). This procedure provides the following relation, containing the parameters α and v, the number of segments N of the polymer, and the critical composition φ_c of the system:

$$\alpha = \frac{\left[6\varphi_c^3(N-1) + \varphi_c^2(11-2N) - 4\varphi_c - 1\right](1-v\varphi_c)^4}{6\varphi_c^2 N\left(1-\varphi_c^2\right)(4v\varphi_c + v - 1)} \tag{63}$$

Plotting α according to (63) as a function the critical composition φ_c for a given polymer (i.e., constant value of N) with v as independent variable gives access to the combination of α and v values, yielding more than one solution for φ_c. Figure 15 shows the results for two v values; this graph merely specifies which parameter combinations result in critical conditions, it does not yet refer to a certain temperature. The horizontal lines indicate the first appearance of an additional critical point upon an augmentation of α. Under these special circumstances, a stable and an unstable critical point [53] coincide and form a double critical point. In the general case, the three solutions for the critical conditions correspond to different temperatures and one of them is an unstable critical point.

The minimum α value required for the occurrence of a double critical point is considerably higher for $v = 0.4$ than for $v = 0.5$. A more detailed mathematical analysis [53] of (63) yields a border line for the combination of parameters, which separates the normal from anomalous behavior. For ordinary systems, the combination of α and v values required to produce multiple critical points has so far not been observed. However, for water/PVME systems, such data may well be realistic

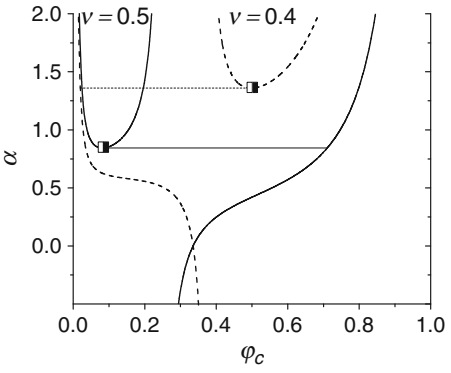

Fig. 15 Modeling of polymer solutions with anomalous phase behavior. Example of plots [53] of α as a function of φ_c according to (63) at the constant v values indicated in the graph for 1. *Solid curves* $v = 0.5$, *dashed curves* $v = 0.4$. The *horizontal lines* mark the minimum value that α must exceed for a given v to generate an additional critical point. S*quares* mark anomalous double critical points

because of the large surface of water as compared with that of the polymer segment, making large γ values and hence also large ν values plausible [cf. (24)]. In view of the pronounced chemical dissimilarities of water and PVME, this should lead to large α values.

The phase diagram shown in Fig. 16 was calculated [53] choosing a combination of α and ν values inside the range of multiple critical points. For this modeling it was (unrealistically but for the sake of simplicity) assumed that only α depends on temperature and that this dependence can be formulated as:

$$\alpha = \alpha_1 + \alpha_2(T - T_s) \tag{64}$$

where α_1, α_2, and T_s are constants. From this graph it is clear that the central features of the phase diagram observed for the water/PVME system can be adequately modeled by the present approach.

An interesting result of the present modeling is an uncommon option to realize theta conditions. Maintaining its definition in terms of $A_2 = 0$, leading to $\chi_o = 0.5$:

$$\chi_{o,\theta} = \frac{1}{2} = \alpha_\theta - (\zeta\lambda)_\theta \tag{65}$$

it is obvious that this relation cannot only be fulfilled in the normal way, with $\zeta_\theta = 0$ and $\alpha_\theta = 1/2$, but also via an adequate combination of α and $\zeta\lambda \neq 0.5$. For such exceptional systems, the unperturbed state results from an exact compensation of an uncommonly unfavorable contact formation between the components ($\alpha > 0.5$) by an extraordinarily advantageous conformational response ($\zeta\lambda \gg 0$). In the case of H_2O/PVME, the plausibility of large α values has already been mentioned. From reports [56] on the formation of a complex between water and PVME and the fact that the system exhibits LCST behavior, one can infer that large ζ values are caused by the very favorable heat effects associated with that process.

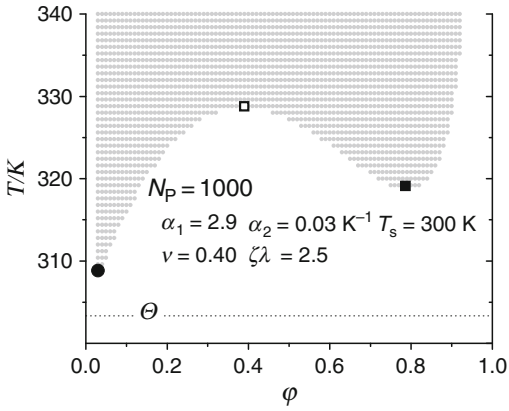

Fig. 16 Spinodal area calculated [53] according to (33) and (64) for an exothermal model system by means of the parameters listed. The *horizontal line* indicates the theta temperature ($\chi_o = 0.5$); *circle* normal critical point, *closed square* stable anomalous critical point, *open square* unstable anomalous critical point

Swelling of Cellulose in Water

The water/cellulose system is unique in several ways. First of all it is so far the only one for which we have observed that the vapor pressures above homogeneous mixtures depend on the particular manner in which the samples were prepared. The results reported here [57] were obtained by means of thin cellulose films (approximately 20–25 μm thick) cast from cellulose solutions in the mixed solvent LiCl + dimethylacetamide. After careful removal of the components of the mixed solvent, these films were kept in a surplus of water at 80°C until the weight of the swollen cellulose film no longer changed. The solvent was then removed stepwise by vacuum treatment and the resulting samples were kept in the measuring cell of the HS–GC until the vapor pressure no longer changed, which was typically after 1 day. The experimental data are highly reproducible but not identical with the results of measurements (of equally reproducibility; not yet published) with cellulose films that were cast from a different solvent. From these findings, one is forced to conclude that at least one set of data does not refer to the macroscopic equilibrium of the system. It looks as if the final arrangement of the polymer chains after total removal of the solvent (e.g., with respect to the degree of crystallinity) could depend on the chemical nature of the solvent employed for film preparation. Under this assumption, and in view of the high viscosity of swollen cellulose, one can then speculate that the molecular environment established upon the removal of a particular solvent is more or less preserved in the swollen state and permits only the establishment of local equilibria.

Figure 17 shows the results for a cellulose sample with 2940 segments (defined by the molecular volume of water) prepared from a solution in LiCl plus dimethylacetamide [57]. The most striking feature is the enormously large range that the Flory–Huggins interaction parameter spans as a function of composition. It falls from $\chi_o = 6$ (for worse than theta conditions, the typical χ_o values are in the order of 0.6) to a minimum of approximately −3.6 (much less than the lowest values observed so far) for φ values around 0.6, and increases again up to −1.7 in the limit of the pure polymer.

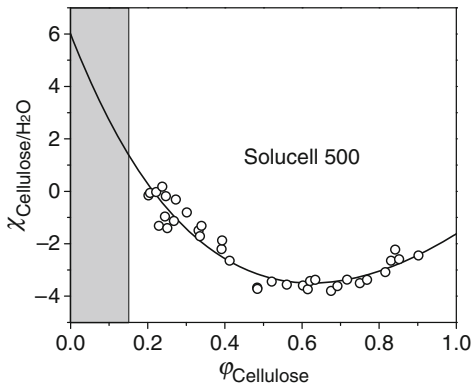

Fig. 17 Composition dependence of the interaction parameter for water/cellulose (Solucell 500) at 80°C, obtained from vapor pressure measurements [57]. The two-phase area is *shaded*. The *curve* was calculated by means of (26) and the following system-specific parameters: $\alpha = 56.8$, $\nu = -0.56$, $\zeta = 37.9$, and $\lambda = 1.34$

For the modeling of the function $\chi(\varphi)$ of Fig. 17, it is essential to use (26) and not (33) because the intramolecular interaction parameter λ deviates strongly from the usual value of 0.5. This observation is conceivable considering the fact that cellulose is not noticeably soluble in water under the prevailing conditions, which means that isolated polymer coils should be widely collapsed. Under these conditions, the average volume fraction Φ_o of the segments within the realm of such a macromolecule will become very high and so consequently will λ [cf. (27) and (17)]. The evaluation of the present data yields $\lambda = 1.34$. All other parameters required for the modeling of the measured Flory–Huggins interaction parameter also lie well outside the normal range. The leading parameter α of the first term of (26) is positive and very large – like with the example of multiple critical points discussed in the previous section (Sect. 4.1.1.4). However, this time the large value is not only due to the chemical dissimilarity of the components, but is also caused by very favorable intersegmental contacts (H-bonds) that must be broken upon the insertion of a solvent. In agreement with the general interrelation of the parameters $\zeta\lambda$ and α, this adverse contribution via α is counteracted by a comparable advantageous conformational relaxation via ζ. The unique behavior of the water/cellulose system is also demonstrated by the value of v, which is negative, in contrast to almost all other polymer solutions studied so far. The only negative value of similar magnitude was observed for the butane/1,4-polybutadiene system [50], which also exhibits a large solubility gap. One might therefore speculate that the pronounced self-association tendencies of the components (due to the unfavorable mutual interaction) causes effective surface-to-volume ratios [cf. (24)] that differ considerably from those expected on the basis of the molecular shapes of the components.

A further, immediately obvious particularity of the present system is the anomalous swelling behavior of cellulose in water, as shown in Fig. 18. To the author's knowledge it is the only case where a high molecular weight polymer takes up more of the pure coexisting liquid than does a sample of lower molar mass.

The results shown in Fig. 18 demonstrate that the miscibility gap of cellulose and water, predicted from the vapor pressures measured above the homogeneous mixture

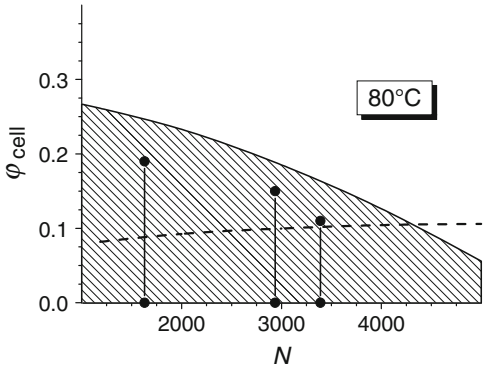

Fig. 18 Composition of the phases coexisting for the system water/cellulose at 80°C as a function of the number of segments N of the polymer determined in swelling experiments [57]. *Symbols* indicate experimental data; the *solid line* was calculated by means of (26) as described in the text; the two phase area is hatched. The *dashed line* (normal behavior) was calculated by means of the original Flory–Huggins theory, setting the interaction parameter equal to 0.54

(liquid/gas equilibrium), matches the observed swelling behavior (liquid/liquid equilibrium) reasonably well. Above all, it correctly models the observed *diminution* of the two-phase region with rising molar mass of the cellulose. The lack of quantitative agreement should not be overestimated because of the sensitivity of the calculated swelling with respect to the exact value of the central parameter α; a reduction of α by less than 3% would suffice for quantitative matching.

In an attempt to rationalize this unique behavior, we recall that the χ_o values of the present system are about ten times larger than normal, which means that the tendency to form dilute solutions is practically nil. When adding increasing amounts of water to pure cellulose, the extent of chain overlap (stabilizing the homogenous state) will surpass a critical value below which a cellulose molecule can no longer evade the formation of extremely adverse contacts between its segments and water. At this point, the segregation of a second phase consisting of practically pure water sets in. From simple considerations concerning the chain-length dependence of the size of polymer coils, one can conclude that this critical overlap will be reached at higher dilution by larger molecular weight samples than by smaller molecular weight samples, thus explaining the anomalous swelling behavior of cellulose in water.

The last two examples have dealt with systems for which the first step is uncommonly unfavorable and goes along with a favorable second step. For the mixtures described in the next section, the opposite is the case: here a very favorable first step is followed by a correspondingly adverse second step.

Aqueous Solutions of Pullulan and Dextran

These systems exhibit a common feature, which becomes noticeable in the primary data, i.e., in the composition dependence of the vapor pressures. Unlike normal polymer solutions, $p(\varphi)$ shows a point of inflection in the region of high polymer contents, as demonstrated in Fig. 19. This peculiarity and the necessity to introduce an additional term in the expression for the integral interaction parameter g [cf. (42)] is interpreted in terms of hydrogen bonds between the monomer units of the polymer, on one hand, and between water and the monomers, on the other hand.

The opening of intersegmental contacts – a prerequisite for the dilution of the mixture – is Gibbs energetically adverse and modeled in terms of positive $\overline{\omega}$ parameters. The subsequent insertion of solvent molecules between these polymer segments is, in contrast, very favorable and quantified by negative α values. The reason why the total contribution of the first step of dilution cannot be modeled by a single common parameter lies in the different composition dependencies of the effects of opening and of insertion.

According to the details of the dilution process discussed above, the point of inflection in the vapor pressure curve shown in Fig. 19 can be given an illustrative meaning: In the region of low polymer concentration it is practically only “bulk” water that it transferred into the vapor phase. This situation changes, however, as φ approaches unity; under these conditions the vapor is increasingly made up of solvent molecules taken from the “bound” water (located between two polymer

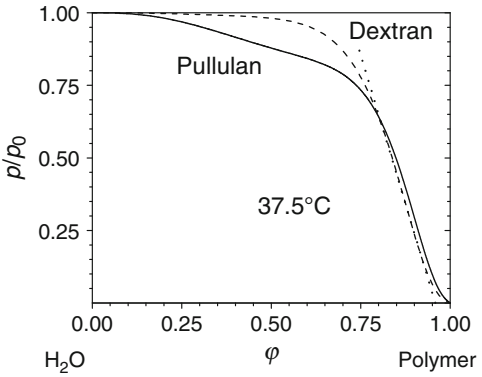

Fig. 19 Comparison of the vapor pressures above aqueous solutions of two types of polysaccharides [26] at 37.5°C calculated by means of (43) plus (5) and (6). The *dotted line* is the tangent at the point of inflection in the case of dextran

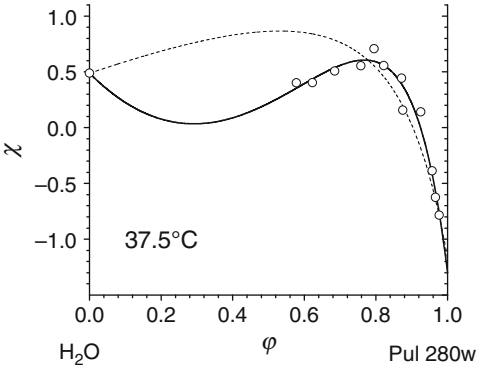

Fig. 20 Composition dependence of the Flory–Huggins interaction parameter for the system [26] water/pullulan at 37.5°C. The *solid line* shows the best fit by means of (43) and the *dotted line* the best fit according to (32)

segments). The intersection of the tangent at the point of inflection with the abscissa can be taken as an estimate of the amount of "bound" water.

Another feature that is immediately visible from Fig. 19 is the higher solvent quality of water for pullulan as compared with dextran. Within the composition range $0.25 > \varphi > 0.75$, the reduced vapor pressure is considerable lower in the former than in the latter case. This situation leads to rather complicated composition dependencies of the Flory–Huggins interaction parameter for the solutions of pullulan, as shown in Fig. 20. From the dotted line of this graph it becomes obvious that a modeling is impossible without an additional term in the relation for the integral interaction parameter (42). The uncommonly low χ values of the system for large volume fraction of the polymer are another outcome of a very stable "intercalation" of a solvent molecule between two segments of the polysaccharide.

Nonselective Solvent/Block Copolymers

The modeling of block copolymers solutions is necessarily much more difficult than the modeling of solutions of random copolymers. Again, the binary system

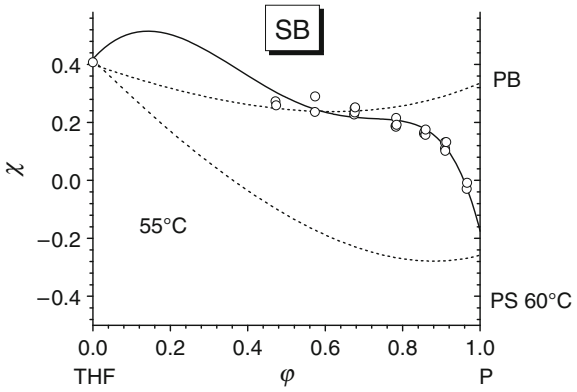

Fig. 21 Composition dependence of the Flory–Huggins interaction parameter for the solutions of a diblock copolymer of styrene and butadiene (*solid line*) in THF at 55°C. The information for the corresponding homopolymer solutions (*dotted lines*) refers to 55°C for PB, and to 60°C for PS [58]

requires three different interaction parameters for its adequate description, but this time a possible incompatibility of the homopolymer blocks is much more consequential. The examples discussed for block copolymers are a diblock copolymer of styrene and butadiene (SB), the corresponding triblock copolymer formed by joining two SB blocks at their butadiene ends (SB)2, and a four-arm block copolymer (SB)4 in which the inner blocks consist of polybutadiene. The investigations reported in [58] use the nonselective tetrahydrofuran (THF) as solvent in all cases. Figure 21 presents – as an example – the composition dependence of the Flory–Huggins interaction parameter measured for the diblock copolymer at 55°C. The results for the other two types of block copolymers and different temperatures look qualitatively very similar.

Like with the aqueous solutions of the polysaccharides discussed in Sect. 4.1.1.6, the present systems require an extra term in the integral interaction parameter g to account for the effect of the first step of dilution, where a solvent molecule is inserted between two polymer segments. With the block copolymers of present interest, the situation is different from that encountered with the polysaccharide solutions because of the microphase separation induced by the incompatibility of the blocks. In this case, the number of segments required for special interactions is larger than two. Geometrical considerations suggest that contacts between more than three segments belonging to different polymer chains are very unlikely, even in the pure melt. This means that the insertion of a solvent molecule will typically destroy advantageous ternary contacts between segments. By analogy to the reasoning in the context of the aqueous solutions of pullulan or dextran, this implies that the extra contribution to g should depend on the third power of φ in the case of block copolymers, as formulated in (44).

Despite these dissimilarities in the molecular details, the α parameters required for the modeling of the experimental findings are in both cases negative. In the case

of the block copolymer solutions, it is not the formation of favorable contacts resulting from the addition of solvent that makes $\alpha < 0$, but the destruction of very unfavorable contacts between the two types of monomeric units. Figure 21 shows that the Flory–Huggins interaction parameter is smallest in the limit of $\varphi \to 1$, where the solvent is practically exclusively incorporated into the interphase separating the coexisting microphases. In this concentration range χ can in some cases even fall below the χ value of the THF/PS system. With progressive dilution, the interaction parameters for the block copolymer increase because the solvent is now more and more incorporated into the microphases until they pass a maximum in the range of semidilute solutions. The reason for this thermodynamically worst situation can be rationalized by the fact that the polymer concentration is no longer high enough to enable microphase separation and not yet low enough for intramolecular clustering of the segments of the different blocks. Maxima in $\chi(\varphi)$ of the type shown in Fig. 21 might cause (macro)phase separation. Calculation for the present copolymer solutions and temperatures under investigation with respect to liquid/liquid demixing by means of (36) and (37) and the interaction parameters obtained from liquid/gas equilibria did not, however, result in miscibility gaps, in agreement with the direct experimental observation of the mixtures. According to these calculations, the thermodynamic quality of THF for the block copolymers is already marginal so that one can expect the occurrence of macrophase separation in addition to microphase separation at low enough temperatures.

Before leaving the area of polymer solutions to deal with polymer blends and mixtures of low molecular weight compounds, it appears worthwhile to document once more an experimental finding that is very helpful for the modeling of new systems. This is the existence of a very general interrelation between the leading parameters α and $\zeta\lambda$ of the present approach. Even for systems that behave in a very anomalous manner at higher polymer concentrations, the parameters α and $\zeta\lambda$ suffice for the description of the dilute state of pair interaction between the solutes and interrelate in the usual way [cf. (34)]. Figure 22 shows the data for the studied polymer solutions with specific interactions, together with some typical data for ordinary polymer solutions that do not need an extension of (32) for the integral interaction parameter. The general validity of the function $\zeta\lambda$ (α) reduces the number of adjustable parameters by one and eases the modeling and qualitative predictions considerably.

4.1.2 Polymer Blends

Poly(vinyl methyl ether)/Polystyrene

Out of the many polymer blends investigated so far, PVME/PS is probably the one for which the molecular weight dependence of the critical conditions has been studied in most detail (cf. citations in [59]). The critical temperatures span more than 60°C, and the critical volume fractions of PS lie between 0.13 and 0.68. The comprehensive experimental information that is available makes this system

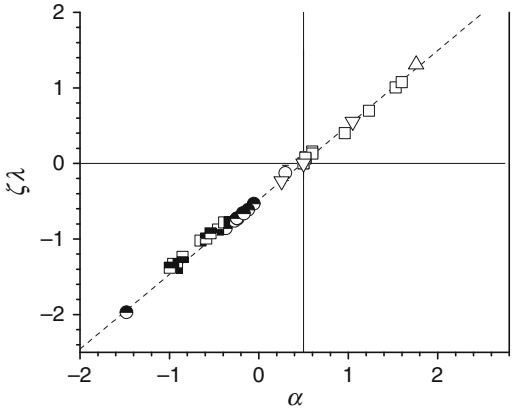

Fig. 22 Interrelation between the parameters $\zeta\lambda$ and α [the *vertical line* at $\alpha = 0.5$ is drawn according to (34)]. The data for solutions of several typical polymers in organic solvents are almost exclusively located in the first quadrant (*open symbols*); they only extend into the third quadrant for systems close to their demixing. Data for anomalous systems (*half-closed symbols*), where the first step of dilution represents the main driving force to homogeneity, are entirely located in the third quadrant

particularly suited for modeling of interaction parameters on the basis of critical conditions.

The modeling presented here still uses the expression for the integral interaction parameter as formulated for polymer *solutions* (26), which leads to the critical conditions specified in (36) and (37). According to the extension of the approach to polymer *blends* (which had not yet been carried out when this study was performed), (49) should have been used for that purpose because it accounts for the fact that the polymer coils A are accessible to the segments of polymer B and vice versa. Both expressions employ a linear dependence of the parameter ζ on the composition of the mixture; the differences between polymer solution and polymer blends only lie in the numerical values of the constants.

Figure 23 shows how the molar masses of the blend components influence the experimentally obtained critical compositions of the mixture. The two curves shown in this graph were obtained by adjusting five parameters, namely v and λ (which were considered to be temperature independent), plus two parameters for the temperature dependence of α. The fifth parameter concerns ζ, which was either kept constant (variant 1) or set proportional to α (variant 2). Both assumptions model the experimental data with comparable accuracy. In view of the expectation that all system-specific parameters should depend on temperature, the quality of the description with only five parameter is surprising. It must, however, be kept in mind that a naive molecular interpretation of the system-specific parameters is not permissible in the present case.

Despite the similarity of the two variants of modeling presented in Fig. 23, the detailed phase diagrams calculated from the two sets of parameters differ

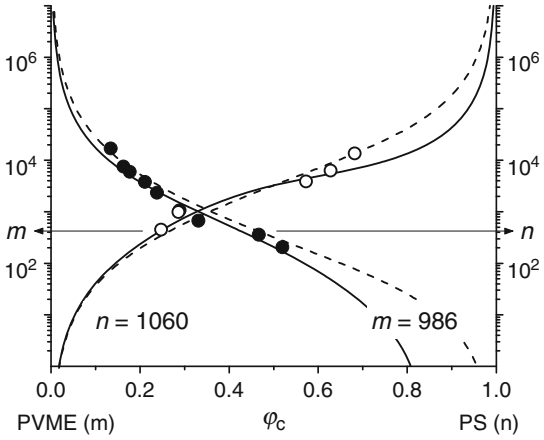

Fig. 23 Combination of numbers m of PVME segments with numbers n of PS segments leading to the critical compositions φ_c. The experimental data, taken from the literature [60–62], were obtained by mixing one PS sample ($n = 1060$, *open circles*) with PVME of different molar mass or, vice versa, one PVME sample ($m = 986$, *closed circles*) with different samples of PS. The *curves* are calculated using two modeling variants as described in the text [59]. *Solid lines*: the conformational relaxation does not depend on temperature; *dashed lines*: it varies linearly with T

fundamentally if both components become high in molar mass. In both variants, α was considered to depend on temperature but variant 1 keeps ζ independent of T, whereas variant 2 applies the proportionality between α and ζ, i.e., treats ζ as a function of T. Variant 1 yields two stable and one unstable critical points [59] (as for the system water/PVME), whereas the demixing behavior remains normal for variant 2. Defining theta conditions for polymer blends by analogy to the usual definition for polymer solutions in terms of critical temperature for infinite molar mass of the polymer according to:

$$\lim_{m,\, n \to \infty} T_c \equiv \Theta \tag{66}$$

one obtains two different theta temperatures, where the corresponding critical concentration is either zero or unity. Conversely, ζ proportional to α yields only one theta temperature, and the corresponding critical composition remains indefinite, like in the original Flory–Huggins theory. The question of which of the predictions comes closer to reality can only be answered by directed experiments.

Shape-Induced Polymer Incompatibility

Demixing of polymer blends consisting of macromolecules synthesized from the same monomers and differing practically only in their molecular architecture plays

an important role in the polyolefin industry [63–65]. Numerous experimental and theoretical studies have therefore been performed to investigate this phenomenon; for pertinent literature see [66]and [67]. The present approach offers a particularly simple theoretical access because the first term of the expression for the integral interaction parameters [(49), corresponding to the first step of mixing] can be set to zero.

For the special case of linear and branched polymers of the same chemistry, one obtains a very simple relation if the degree of branching β is introduced in terms of the intrinsic viscosity of the branched polymer as compared with that of the linear analog [(27) and (52)] and the conformational relaxation is set proportional to β (53), which means that it approaches zero as the degree of branching becomes vanishingly small. Under these conditions, one single parameter suffices to model the phase behavior (54); the parameter κ of (54) can either be estimated from the Kuhn–Mark–Houwink relation for the linear polymer and theta conditions [(29) and (55)] or it can be merged with the parameter Z (54). Figure 24 shows an example of the critical conditions calculated for blends of chemically identical linear and branched polymers with $\kappa = 0.27$, which is the typical value for vinyl polymers.

Model calculations [28] along the described lines indicate that the sensitivity to phase separation is particularly pronounced for blend partners of comparable numbers of segments. In Fig. 24 this can, for instance, be seen from the frontmost curve ($\beta = 0.1$) passing a maximum in this range of N_L. Each of the data points on the critical surface of this graph corresponds to a different phase diagram, which can be represented in terms of $Z(\varphi)$, by analogy to the more customary theoretical diagrams $\chi(\varphi)$ or $g(\varphi)$. In order to transform such general phase diagrams into the directly measurable phase diagrams $T(\varphi)$ (phase separation temperatures as function of composition), it is necessary to know how the parameters Z, χ, or g depend on T. There are literature reports [65] on phase separation upon heating as well as

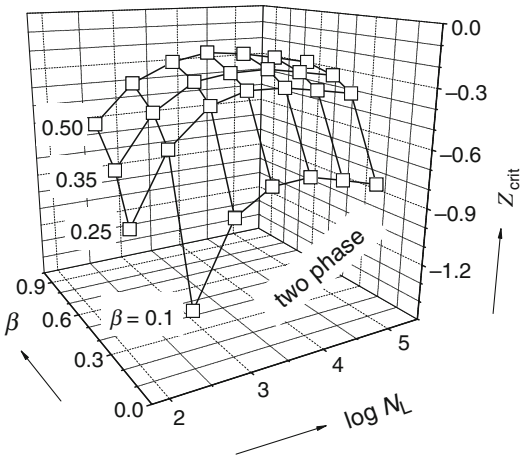

Fig. 24 Three-dimensional representation of the critical surface calculated for blends of a branched polymer consisting of 1000 segments but differing in its degrees of branching β, with its linear analogs varying in the number N_L of their segments. Phase separation may set in (depending on the composition of the blend) if Z falls below its critical value Z_{crit}. The area of possible demixing is located below the critical surface [28]

upon cooling. In view of the fact that the first term of (49) is for the present calculations set at zero ($\alpha = 0$), one might think that shape-induced demixing should be entirely due to unfavorable entropies of mixing and should always be of the LCST type. This interpretation is, however, not permissible because both steps of dilution contribute to the residual Gibbs energy via enthalpy and entropy, as discussed earlier.

4.1.3 Mixtures of Low Molecular Weight Liquids

For the modeling of systems containing more than one low molecular weight component, like polymer solutions in mixed solvents, it would be very advantageous to be able to use the same mathematical expressions for the mixtures of the low molecular weight liquids. Experiments performed to investigate these possibilities have demonstrated that (32) can indeed describe the thermodynamic behavior quantitatively [29], as demonstrated in Fig. 25 for the system water/*N*-methyl morpholin *N*-oxide monohydrate [NNMO*H_2O]. This graph shows the measured reduced vapor pressures of water as a function of composition, and the curves calculated by means of (32) and the adjusted parameters α, ν, and $\zeta\lambda$.

It is obvious that the parameter λ of (32) (introduced via considerations concerning the establishment of microphase equilibria with polymer-containing systems) loses its physical meaning for the low molecular weight mixtures because the segments of the components are geometrically strictly separated. This is unlike the situation with polymer solutions, where the solvent enters the polymer coil, or

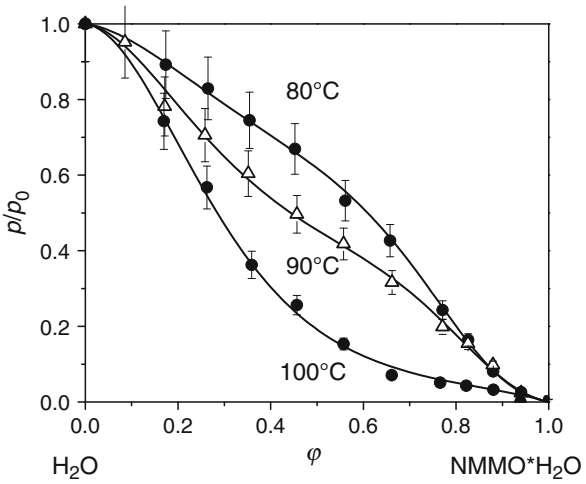

Fig. 25 Equilibrium vapor pressures, p, of water above mixtures of NMMO*H_2O normalized to p_o, the equilibrium vapor pressure of pure water, as a function of the volume fraction of NMMO hydrate for the indicated temperatures [29]. The *curves* are calculated according to (32), where $N_{NMMO*H_2O} = 6.35$

with polymer blends, where both components are accessible for segments of the other polymer. The meaning of the parameter ζ, on the other hand, remains unchanged because molecular rearrangements, similar to those occurring with polymer solutions and polymer blends, will also take place in low molecular weight mixtures, due to preferentially interacting sites of the components. According to the present results, a linear composition dependence of the conformational part of the interaction parameter should suffice to describe reality.

4.2 Ternary Systems

The material presented so far has demonstrated the ability to model the thermodynamic behavior of binary systems accurately by means of the present approach. For the description of polymer solutions, it is normally possible to eliminate one of the three parameters of (32) thanks to a general interrelation between α and $\zeta\lambda$ (34). For polymer blends and mixtures of low molecular weight components, a similar general simplification is presently not known. Notwithstanding this situation, it is possible to model the principle features [27] of all types of phase diagrams observed for ternary systems using only two parameters for each binary subsystem.

This section deals with the phase-separation behavior of ternary systems, where a distinction is made between polymer solutions in mixed solvents (Sect. 4.2.1) and solutions of two polymers in a single solvent (Sect. 4.2.2). Furthermore, the systems are classified according to the way the thermodynamic properties of the ternary systems are made up from the properties of the corresponding binary subsystems: *Simplicity* denotes "smooth" changes in the phase behavior of the binary subsystems upon the addition of the third component in its pure form or in mixtures (see later). *Cosolvency* means that the thermodynamic quality of mixture of two components is higher with respect to the third component than expected by simple additivity, i.e., cosolvency reduces the extension of the two-phase region with respect to that expected from additivity. *Cononsolvency*, finally, denotes the opposite behavior, i.e., an extension of the two-phase region beyond expectation.

4.2.1 Mixed Solvents

The use of mixed solvents is widespread, because it offers the possibility to tailor desirable thermodynamic conditions by mixing two liquids with sufficiently different qualities in adequate ratios, instead of the often inconvenient or even impossible variation of temperature. The combination of good solvents with precipitants is the basis of many industrial processes, like membrane production or fiber spinning. In order not to go beyond the scope of the present contribution, the following considerations are limited to complete miscibility of the components of the mixed solvent. There is, however, no particular difficulty to extend the treatment to incompletely miscible components of mixed solvents.

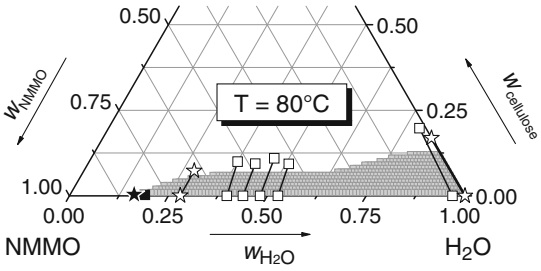

Fig. 26 Phase diagram of the NMMO/H_2O/Solucell 400 system at 80°C [68]. *Shaded area* shows the calculated unstable composition range; *open squares* calculated tie lines, *open stars* experimental tie lines, *closed square* calculated critical point, *closed star* experimental critical point

Simplicity

The following example for simplicity refers to a technically important ternary system, namely cellulose solutions in mixtures of the favorable solvent NMMO with the precipitant water. Fibers are formed as thin threads as homogeneous cellulose solutions are spun into water. Figure 26 shows how experimental data for this ternary mixture compares with the modeling [68] on the basis of (60). On the theoretical side, it is important to take care of the fact that the information concerning the binary subsystems usually differs by a diverging definition of the size of a segment.

The unstable area, the critical point, and the tie lines shown in Fig. 26 were calculated by means of the independently determined parameters for the binary subsystems NMMO/water [29] and cellulose/water [57]. The corresponding information for NMMO/cellulose is inaccessible along the present routes, because the vapor pressure of both components is negligibly small. For that reason, it was necessary to adjust the parameters α and ζ for this binary subsystem to the experimentally observed ternary phase diagram; ν was equated to γ (obtained from group contributions) and λ was set at 0.5, the typical value for polymer solutions. This procedure enables the modeling of the phase diagram for the ternary system, which matches the measurements within experimental error. Even if this procedure is not predictive, it helps the discrimination of metastable and unstable compositions and enables assessment of the effects of different molar masses of cellulose on demixing [68].

In another, very abundant form of simplicity the miscibility gaps existing for the polymer solution in either of the two solvents transform smoothly into each other as the composition of the mixed solvent changes.

Cosolvency

A much higher quality of mixed solvents as compared with either of its components is not uncommon; since the first report [69] it has been described in the literature many times. This phenomenon can be easily modeled [27] by means of (60) using physically meaningful combinations of parameters. The example shown in Fig. 27

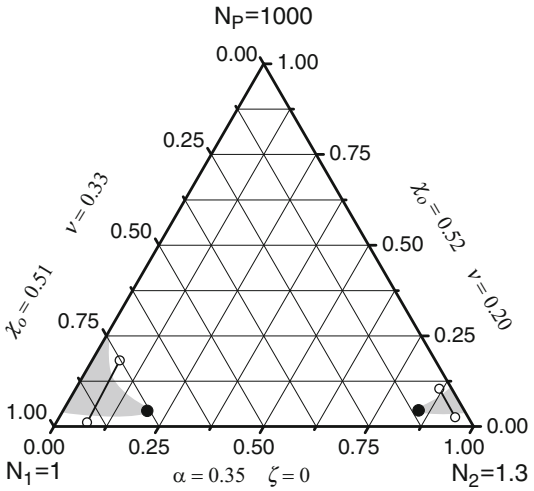

Fig. 27 Cosolvency as a result of unfavorable interactions between components 1 and 2. The numbers of segments of the different components are given at the *corners* of the phase diagram and the characteristic parameters for the binary subsystems are indicated on its *edges*. *Open symbols* composition of coexisting phases, *closed symbols* critical points, *shaded areas* unstable regions [27]

applies to sufficiently unfavorable 1/2 interactions; in their absence the miscibility gap would extend from one binary subsystem to the other throughout the ternary system, i.e., this would be an example of simplicity.

The reason for the complete miscibility of the polymer with mixed solvents containing comparable fractions of their components shown in Fig. 27 lies in the adverse interactions between them. Within a certain range of compositions, the ternary system can avoid these unfavorable contacts between components 1 and 2 by inserting a polymer segment between them and forming homogeneous mixtures.

Cononsolvency

The creation of a miscibility gap by mixing two favorable solvents was reported a long time ago [70] and many examples have been described since. Figure 28 shows a typical modeling of this behavior. For that purpose, we assume that the components 1 and 2 are markedly better solvents for the polymer P than in the case of cosolvency, and that they mix in a combinatorial manner ($g_{12} = \chi_{12} =; 0$).

The reason why the present combination of parameters for the binaries leads to a miscibility gap for the ternary system lies in the particularly favorable interactions 1/P and 2/P as compared with the more or less "neutral" interactions 1/2. Under these conditions, the Gibbs energy of the total system can be lowered by phase separation such that the polymer-lean phase contains practically low molecular weight components only and that many favorable 1/P and 2/P contacts can be formed in the polymer-rich phase.

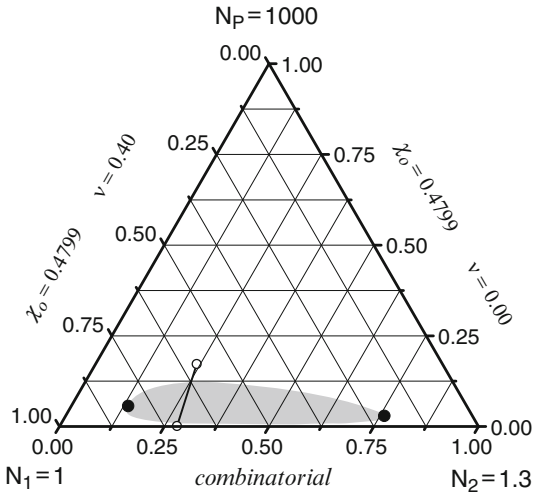

Fig. 28 Formation of an island of immiscibility in the ternary system, caused by favorable 1/P and 2/P interactions [27]. For details, see legend to Fig. 27

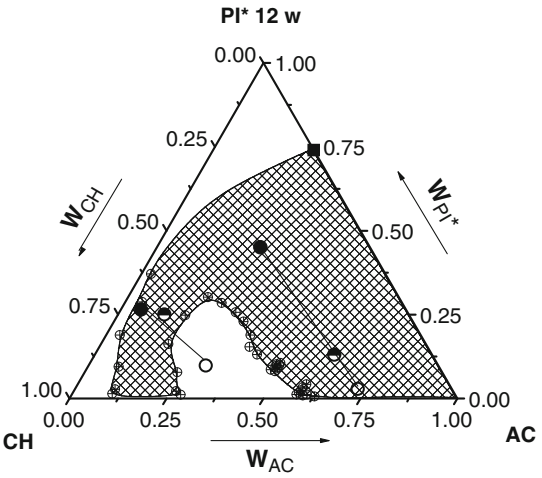

Fig. 29 Phase diagram of the CH/AC/PI* system at 25°C. The polymer sample PI* (M_n = 5 kg/mol, M_w = 12 kg/mol) consists of a mixture of branched and linear chains. *Crossed circles* cloud points, *half-closed circles* overall composition of the coexistence experiments, *open circles* compositions of the polymer-lean phases, *closed circles* compositions of the polymer-rich phases, *closed square* swelling point of PI* in AC. The composition area of possible demixing is *hatched* [71]

Complex Behavior

Phase diagrams for polymer solutions in mixed solvents can look much more complicated than shown so far. Figure 29 gives an example observed in the course of a study concerning differences in the thermodynamic behavior of branched as compared with linear polymers [71].

The reason for uncommon phase diagram often lies in the polydispersity of the polymer sample, which means that we are strictly speaking no longer dealing with ternary but with multinary systems, for which the representation of phase diagrams requires a projection into a plane. In the present case, the polydispersity is due to the

presence of linear and branched PI in addition to the usual nonuniformity of molar masses. The consequences of broad molecular weight distributions of linear polymers for the shape of phase diagrams are not negligible, but are usually considerably less pronounced than nonuniformities with respect to the molecular architecture of the macromolecules. The reason is that polymers of different chain length are usually completely miscible, whereas this needs not be the case for linear and branched macromolecules, as exemplified when dealing with their solutions in a common solvent.

The strange peninsular of the miscibility gap shown in Fig. 29 is caused by the fact that the PI sample contains both linear and branched material; neither the solution of the linear product nor that of the branched polymer in the same mixed solvent show this particularity [71]. It is, however, very probable that particular interactions between the components of the mixed solvent also play a role in the occurrence of the anomalous peninsula of the phase diagram. This consideration rests on the fact that the CH/AC system exhibits an upper critical solution temperature [72] at −29°C. The low mixing tendency of these components might increase the possibilities of the quaternary system to reduce its Gibbs energy via demixing.

4.2.2 Blend Solutions

Solutions of chemically dissimilar polymers in a common solvent play an important role in the processing of polymer mixtures, where this is particularly true for incompatible polymer pairs but also for the production of homogeneous films consisting of two compatible polymers. Like with polymer solutions in mixed solvents, one can observe all the deviations from additive behavior discussed earlier.

Simplicity

The modeled example given in Fig. 30 for this behavior shows the gradual disappearance of a miscibility gap existing between two moderately incompatible polymers upon the addition of a solvent of comparatively low thermodynamic quality.

The phase diagram of Fig. 30 looks very similar to the one measured for the solutions of linear and branched PI in CH and shown in Fig. 31. For these experiments, the originally synthesized branched material (PI* of Fig. 29) was to a large extent freed from the linear components by means of the large-scale method of spin fractionation [73]. Despite the fact that the boundary between the homogeneous and the two-phase area was only mapped, instead of the usual cloud point measurements, the results of Fig. 31 testify to the existence of shape-induced incompatibility of polymers. It is remarkable that this phenomenon can be observed for comparatively low molar masses of the components.

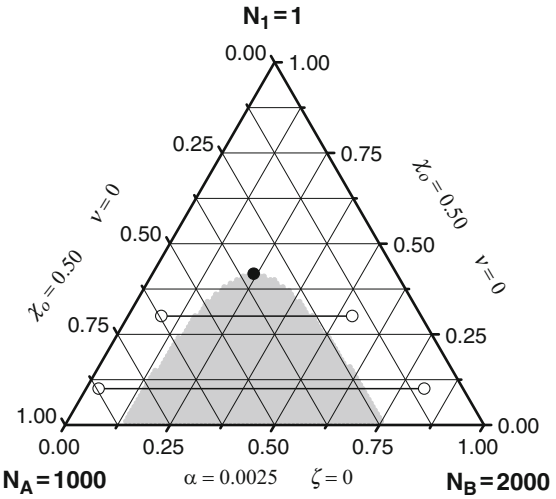

Fig. 30 Phase diagram for a moderately incompatible polymer pair and a solvent of moderate quality that dissolves polymer A and polymer B equally well. *Open symbols* composition of coexisting phases, *closed symbol* critical point, *shaded area* unstable region [27]

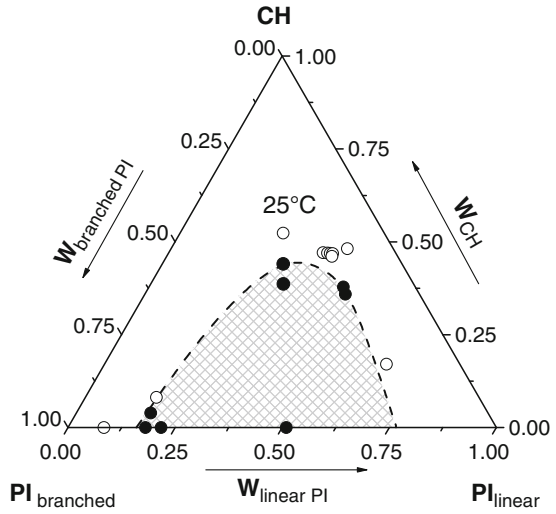

Fig. 31 Phase diagram of the CH/branched PI/linear PI system at 25°C obtained by mapping homogeneous (*open symbols*) and inhomogeneous (*closed symbols*) mixtures. The M_w of the linear polymer is 21.6 kg/mol and that of the branched material is 18 kg/mol. The two-phase region is *hatched* [71]

Cosolvency

According to model calculations, the phenomenon of cosolvency should also occur for solutions of polymer blends in a common solvent. For the example shown in Fig. 32, the components of the blend were chosen to be highly incompatible, and the solvent to be bad for polymer B but favorable for polymer A.

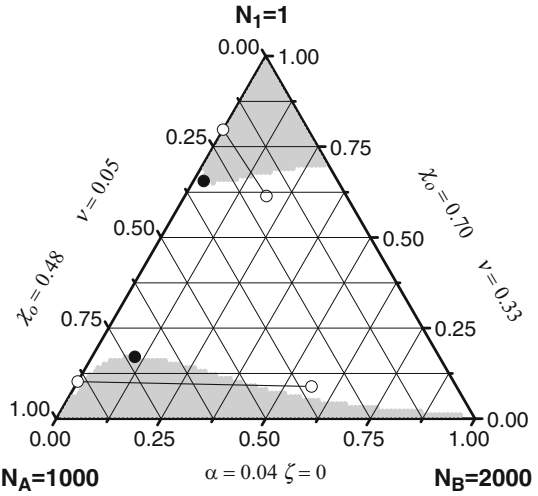

Fig. 32 Phase diagram calculated according to (60) by means of the parameters indicated on the *edges* of the triangle for the ternary mixture solvent 1/polymer A/polymer B. *Open symbols* composition of coexisting phases, *closed symbols* critical points, *shaded areas* unstable regions [27]

As with the example presented for cosolvency in the case of polymer solutions in mixed solvents (Fig. 27), the origin of cosolvency for polymer blends in a common solvent can be interpreted as a dissection of a miscibility gap that would normally bridge the Gibbs phase triangle from one binary subsystem to the other binary system (here from 1/B to A/B) by special interactions between the completely miscible components (here 1/A). With the example of Fig. 32, the thermodynamic quality of the solvent for polymer A is almost marginal; in this manner polymer B becomes completely miscible with certain solutions of polymer A in solvent 1.

Cononsolvency

This phenomenon is generally characterized by the existence of islands of immiscibility inside the Gibbs phase triangle, i.e., phase separation is absent for all binary mixtures. According to model calculations along the present lines, closed miscibility gaps should be comparatively abundant for solutions of two favorably interacting polymers in a common solvent that is sufficiently favorable for both polymers; Fig. 33 shows an example of the outcome of such calculations. A slight modification of the binary interaction parameters for the polymer solutions changes the size of the miscibility gap and its location inside the Gibbs phase triangle considerably. This is, for instance, made evident by the fact that the island disappears by increasing both χ_o values from 0.482 to 0.483, i.e., a slight reduction in the thermodynamic quality of the solvent brings the polymer solutions closer to phase separation.

The explanation for the occurrence of islands of immiscibility under the conditions specified in Fig. 33 lies in the high preference of 1/A and 1/B contacts over A/B contacts (even if A and B interact favorably), as demonstrated by the

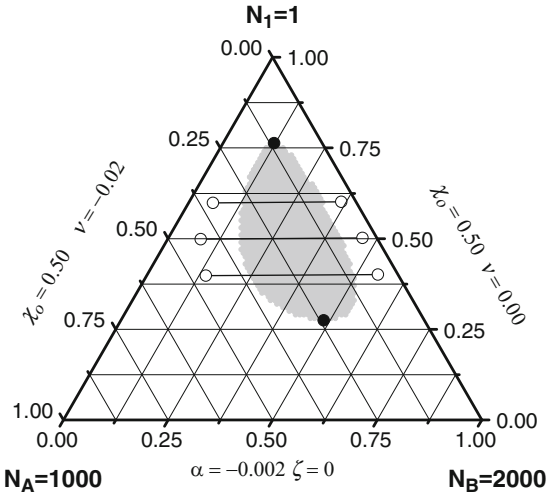

Fig. 33 Phase diagram calculated under the assumption that the polymers A and B are compatible and that the solvent is moderately favorable for both A and B [27]

position of the tie lines. Under these circumstances, the Gibbs energy of the ternary system can be reduced as compared with the homogeneous mixture by forming two liquid phases, one preferentially containing polymer A and the other polymer B. This phase separation leads to a reduction in the number of A/B contacts (associated with lower entropies of mixing than the corresponding 1/A and 1/B contacts) and in a corresponding increase in number of the more favorable polymer/solvent contacts.

The predictions of model calculations of the type shown in Fig. 33 were checked [74] by means of the systems THF/PS/PVME and CH/PS/PVME. This choice was made because of the availability of the thermodynamic information for all binary subsystems. One of the questions to be answered by this comparison between theory and experiment concerns the extent to which the phase behavior of the ternary system can be predicted if the corresponding information for the binary subsystems is available.

Figure 34 shows how experiment and the prediction by means of (60) compare in the case of THF; the data for THF/PS and THF/PVME were taken from [75] and that for the polymer blend from [59].

It is obvious from Fig. 34 that the modeling predicts the phenomenon of cononsolvency but fails to capture the details of demixing. The extension of the calculated island is considerably larger than experimentally observed. If the solvent THF is replaced by CH (which is less favorable for both polymers), the extension of the measured island is considerably increased. Again, the modeling does predict an island, but its size and location in the phase triangle are at variance with reality.

From these results, it must be concluded that the interaction between two chemically different segments is influenced by the vicinity to a segment of the third component. In other words, it is necessary to account for ternary interaction

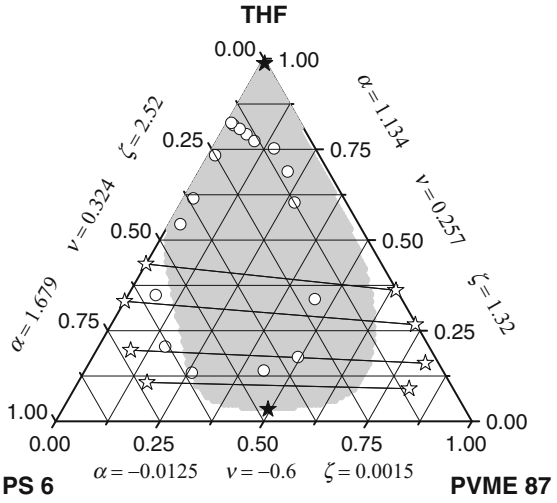

Fig. 34 Measured and calculated phase diagram for the THF/PS/PVME system at 20°C. *Circles* show measured cloud points. The modeling was performed by means of (60) and the binary parameters are shown on the *edges* of the triangle. The calculated spinodal area is *shaded*. *Open stars* composition of the coexisting phases, *closed stars* critical points [74]

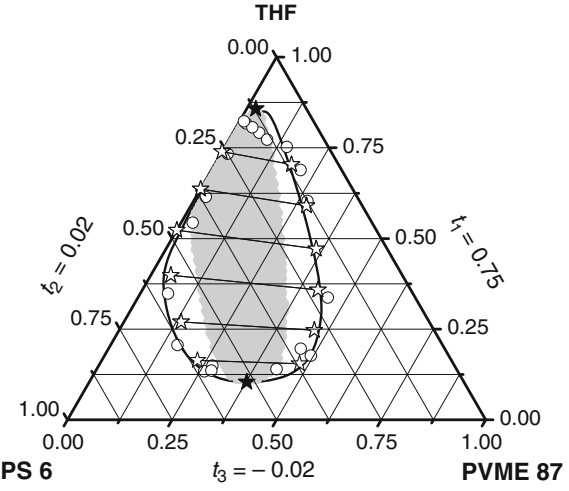

Fig. 35 Phase diagram of the PS/PVME/THF system at 20°C. *Circles* measured cloud points, *closed stars* calculated critical points, *open stars* calculated tie lines. The values of the specific ternary interaction parameters (61) are indicated on the *edges*; the binary interaction parameters are the same as in Fig. 34 [74]

parameters. Figure 35 shows the experimentally determined phase behavior of the system THF/PS/PVME at 20°C, again along with the results of model calculations on the basis of (61) and (60) by means of the ternary interaction parameters stated at the edges of the triangle.

The agreement between the actually measured demixing behavior and that modeled on the basis of binary interaction parameters plus composition-independent ternary interaction parameters is surprisingly good. However, the results also demonstrate how sensitive the calculated phase diagrams can be with respect to the details of some interaction parameters. For instance, the analogous experiments

performed with CH (less favorable solvent) instead of THF using a molecularly disperse PS sample require at least one composition-dependent ternary interaction parameter for their modeling. Indications exist that this complication is due to the presence of PS molecules differing markedly in their molar mass.

One important consequence of the results presented for solutions of compatible polymers in a common solvent is this: The suggested idea to prepare homogeneous polymers films containing both types of macromolecules from joint solutions by solvent evaporation will probably not work. The reason is that solutions containing comparable amounts of polymers A and B need to pass the unstable area of the phase diagram upon the removal of solvent, which means that they inevitably demix into two phases: one rich in polymer A and the other in polymer B. Despite the fact that the system enters the one-phase region again as the solvent content falls below a certain value, the high viscosity of the coexisting liquids will normally prevent homogenization.

5 Conclusions

The theoretical concepts presented in this chapter and the experimental examples given for their validity demonstrate how the Flory–Huggins theory can be made practical with reasonable effort. The central features of the approach are the provision for chain connectivity in dilute polymer-containing systems (by means of microphase equilibria) and the variability of macromolecules with respect to their spatial extension (expressed in terms of conformational relaxation after mixing). Both particularities contribute to the Flory–Huggins interaction parameters and are quantified in a second, additive term, which becomes zero for most of the theta systems. In contrast to the original Flory–Huggins theory, the interaction parameters are no longer independent of concentration; complicated functions $\chi(\varphi)$ are sometimes necessary to model experimental data, including minima and maxima in this dependence. It is therefore no wonder that several parameters are needed to gather the particularities of a certain system. In many cases, two parameters suffice for the quantitative description because of some possible simplifications and interrelations, as described in Sect. 2. With complex systems (like water/cellulose) up to four parameters might, however, be required.

There is one finding that speaks strongly for the validity of the present approach, namely the fact that several types of phase equilibria can be described quantitatively by means of the same set of parameters (cf. the systems *n*- C_4/1,4-PB and $CHCl_3$/PEO). Another eminent advantage of the present approach is its general applicability to very different classes of polymers (including branched macromolecules and copolymers of different architecture); furthermore, there is no obvious reason why it should fail for multicomponent systems.

So far, the extension of the Flory–Huggins theory has enabled the modeling of several hitherto unexplainable anomalous phenomena, like uncommon molecular weight dependencies of second osmotic virial coefficients, the existence of multiple critical points for binary systems, or the odd swelling behavior of cellulose in water.

Furthermore, it has helped a better understanding of ternary mixtures with respect to the conditions that the subsystems must fulfill for the occurrence of cosolvency or cononsolvency, as well as concerning the necessity for the use of ternary interaction parameters. Suggested further investigations concern mixtures containing charged macromolecules and a more detailed analysis of the predictive power of the present approach.

Acknowledgments The author is grateful to Dr. John Eckelt (WEE-Solve AG, Mainz, Germany) and to Prof. Spiros Anastasiadis (University of Crete, Greece) for their constructive criticism, which has certainly improved the readability of this contribution.

References

1. Flory PJ (1953) Principles of polymer chemistry. Cornell Univ. Press, Ithaca
2. Simha R, Somcynsky T (1969) On statistical thermodynamics of spherical and chain molecule fluids. Macromolecules 2(4):342–350
3. Trappeniers NJ, Schouten JA, Ten Seldam CA (1970) Gas–gas equilibrium and the two-component lattice-gas model. Chem Phys Lett 5(9):541–545
4. Sanchez IC, Lacombe RH (1976) An elementary molecular theory of classical fluids. Pure fluids. J Phys Chem 80:2352
5. Dee GT, Walsh DJ (1988) A modified cell model equation of state for polymer liquids. Macromolecules 21(3):815–817
6. Beret S, Prausnitz JM (1975) Perturbed hard-chain theory – equation of state for fluids containing small or large molecules. AIChE J 21(6):1123–1132
7. Chapman WG, Gubbins KE, Jackson G, Radosz M (1989) SAFT – equation-of-state solution model for associating fluids. Fluid Phase Equilib 52:31–38
8. Hino T, Song YH, Prausnitz JM (1994) Liquid–liquid equilibria for copolymer mixtures from a perturbed hard-sphere-chain equation of state. Macromolecules 27(20):5681–5690
9. Fredenslund A, Jones RL, Prausnitz JM (1975) Group-contribution estimation of activity-coefficients in nonideal liquid-mixtures. AIChE J 21(6):1086–1099
10. Heil JF, Prausnitz JM (1966) Phase equilibria in polymer solutions. AIChE J 12(4):678–685
11. Vimalchand P, Donohue MD (1989) Comparison of equations of state for chain molecules. J Phys Chem 93(10):4355–4360
12. De Sousa HC, Rebelo LPN (2000) A continuous polydisperse thermodynamic algorithm for a modified Flory–Huggins model: the (polystyrene plus nitroethane) example. J Polym Sci B Polym Phys 38(4):632–651
13. Chang TS (1939) The number of configurations in an assembly and cooperative phenomena. Proc Cambridge Philos Soc 35:265
14. Flory PJ (1941) Thermodynamics of high polymer solutions. J Chem Phys 9:660
15. Flory PJ (1942) Thermodynamics of high polymer solutions. J Chem Phys 10:51
16. Huggins ML (1941) Solutions of long chain compounds. J Chem Phys 9:440–440
17. Huggins ML (1942) Theory of solutions of high polymers. J Chem Phys 46:151
18. Horst R (1995) Calculation of phase diagrams not requiring the derivatives of the Gibbs energy demonstrated for a mixture of two homopolymers with the corresponding copolymer. Macromol Theory Simulat 4:449
19. Horst R (1996) Calculation of phase diagrams not requiring the derivatives of the Gibbs energy for multinary mixtures. Macromol Theory and Simulat 5:789
20. Horst R (1998) Computation of unstable binodals not requiring concentration derivatives of the Gibbs energy. J Phys Chem B 102(17):3243

21. Koningsveld R, Stockmayer WH, Nies E (2001) Polymer phase diagrams. Oxford University Press, Oxford
22. Flory PJ, Mandelkern L, Kinsinger JB, Shultz WB (1952) Molecular dimensions of polydimethylsiloxanes. J Am Chem Soc 74:3364
23. Wolf BA (2003) Chain connectivity and conformational variability of polymers: clues to an adequate thermodynamic description of their solutions II: Composition dependence of Flory–Huggins interaction parameters. Macromol Chem Phys 204:1381
24. Eckelt J, Samadi F, Wurm F, Frey H, Wolf BA (2009) Branched versus linear polyisoprene: Flory–Huggins interaction parameters for their solutions in cyclohexane. Macromol Chem Phys 210:1433
25. Bercea M, Eckelt J, Wolf BA (2008) Random copolymers: their solution thermodynamics as compared with that of the corresponding homopolymers. Ind Eng Chem Res 47:2434
26. Eckelt J, Sugaya R, Wolf BA (2008) Pullulan and dextran: uncommon composition dependent Flory–Huggins interaction parameter of their aqueous solutions. Biomacromolecules 9:1691
27. Wolf BA (2009) Binary interaction parameters, ternary systems: realistic modeling of liquid/liquid phase separation. Macromol Theory Simulat 18:30
28. Wolf BA (2010) Polymer incompatibility caused by different molecular architectures: modeling via chain connectivity and conformational relaxation. Macromol Theory Simulat 19:36
29. Eckelt J, Wolf BA (2008) Thermodynamic interaction parameters for the system water/NMMO hydrate. J Phys Chem B 112:3397
30. Tanaka TE (2000) Experimental methods in polymer science. Academic, New York
31. Petri H-M, Wolf BA (1994) Concentration dependent thermodynamic interaction parameters for polymer solutions: quick and reliable determination via normal gas chromatography. Macromolecules 27:2714
32. Krüger K-M, Sadowski G (2005) Fickian and non-Fickian sorption kinetics of toluene in glassy polystyrene. Macromolecules 38:8408
33. Ninni L, Meirelles AJA, Maurer G (2005) Thermodynamic properties of aqueous solutions of maltodextrins from laser-light scattering, calorimetry and isopiestic investigations. Carbohydr Polym 59(3):289
34. Karimi M, Albrecht W, Heuchel M, Weigel T, Lendlein A (2008) Determination of solvent/polymer interaction parameters of moderately concentrated polymer solutions by vapor pressure osmometry. Polymer 49(10):2587–2594
35. Gao ZN, Li JF, Wen XL (2002) Vapor pressure osmometry and its applications in the osmotic coefficients determination of the aqueous monomer glycol and polymer polyethylene glycol solutions at various temperature. Chin J Chem 20(4):310–316
36. Eliassi A, Modarress H, Nekoomanesh M (2002) Thermodynamic studies of binary and ternary aqueous polymer solutions. Iran J Sci Technol 26(B2):285–290
37. Schreiber HP (2003) Probe selection and description in Igc: a nontrivial factor. J Appl Polym Sci 89(9):2323–2330
38. Voelkel A, Strzemiecka B, Adamska K, Milczewska K (2009) Inverse gas chromatography as a source of physiochemical data. J Chromatogr A 1216(10):1551–1566
39. Bercea M, Cazacu M, Wolf BA (2003) Chain connectivity and conformational variability of polymers: clues to an adequate thermodynamic description of their solutions I: Dilute solutions. Macromol Chem Phys 204:1371
40. Petri H-M, Schuld N, Wolf BA (1995) Hitherto ignored influences of chain length on the Flory–Huggins interaction parameter in highly concentrated polymer solutions. Macromolecules 28:4975
41. Bercea M, Wolf BA (2006) Vitrification of polymer solutions as a function of solvent quality, analyzed via vapor pressures. J Chem Phys 124(17):174902–174907
42. Wolf BA, Adam HJ (1981) Second osmotic virial coefficient revisited – variation with molecular weight and temperature from endo- to exothermal conditions. J Chem Phys 75:4121
43. Schotsch K, Wolf BA, Jeberien H-E, Klein J (1984) Concentration dependence of the Flory–Huggins parameter at different thermodynamic conditions. Makromol Chem 185:2169

44. Bercea M, Wolf BA (2006) Enthalpy and entropy contributions to solvent quality and inversions of heat effects with polymer concentration. Macromol Chem Phys 207(18):1661–1673
45. Saeki S, Kuwahara S, Konno S, Kaneko M (1973) Upper and lower critical solution temperatures in polystyrene solutions. Macromolecules 6(2):246
46. Stryuk S, Wolf BA (2003) Chain connectivity and conformational variability of polymers: clues to an adequate thermodynamic description of their solutions III: Modeling of phase diagrams. Macromol Chem Phys 204:1948
47. Schuld N, Wolf BA (1999) Polymer–solvent interaction parameters In: Brandrup J, Immergut EH, Grulke EA (eds) Polymer handbook, 4th edn. Wiley, New York
48. Krigbaum WR, Geymer DO (1959) Thermodynamics of polymer solutions. The polystyrene–cyclohexane system near the Flory theta temperature. J Am Chem Soc 81:1859
49. Wolf BA, Jend R (1977) Über die Möglichkeiten zur Bestimmung von Mischungsenthalpien und -volumina aus der Molekulargewichtsabhängigkeit der kritsichen Entmischungstemperaturen und -drucke. Makromol Chem 178:1811
50. Stryuk S, Wolf BA (2005) Liquid/gas and liquid/liquid phase behavior of n-butane/1,4-polybutadiene versus n-butane/1,2-polybutadiene. Macromolecules 38(3):812
51. Sanchez IC, Balazs AC (1989) Generalization of the lattice-fluid model for specific interactions. Macromolecules 22:2325
52. Khassanova A, Wolf BA (2003) PEO/CHCl: crystallinity of the polymer and vapor pressure of the solvent – equilibrium and non-equilibrium phenomena. Macromolecules 36(17):6645
53. Wolf BA (2005) On the reasons for an anomalous demixing behavior of polymer solutions. Macromolecules 38(4):1378
54. Šolc K, Dušek K, Koningsveld R, Berghmans H (1995) "Zero" and "off-zero" critical concentrations in solutions of polydisperse polymers with very high molar masses. Collect Czech Chem Commun 60(10):1661–1688
55. Schäfer-Soenen H, Moerkerke R, Berghmans H, Koningsveld R, Dušek K, Šolc K (1997) Zero and off-zero critical concentrations in systems containing polydisperse polymers with very high molar masses. 2. The system water-poly(vinyl methyl ether). Macromolecules 30(3):410–416
56. Meeussen F, Bauwens Y, Moerkerke R, Nies E, Berghmans H (2000) Molecular complex formation in the system poly(vinyl methyl ether)/water. Polymer 41(10):3737–3743
57. Eckelt J, Wolf BA (2007) Cellulose/water: l/g and l/l phase equilibria and their consistent modeling. Biomacromolecules 8:1865
58. Xiong X, Eckelt J, Zhang L, Wolf BA (2009) Thermodynamics of block copolymer solutions as compared with the corresponding homopolymer solutions: experiment and theory. Macromolecules 42:8398
59. Wolf BA (2006) Polymer–polymer interaction: consistent modeling in terms of chain connectivity and conformational response. Macromol Chem Phys 207(1):65
60. Halary JL, Ubrich JM, Monnerie L, Yang H, Stein RS (1985) Polym Commun 26:73
61. Ben Cheikh Larbi F, Lelong S, Halary JL, Monnerie L, Yang H (1986) Polym Commun 22:23
62. Rätsch MT, Kehlen H, Wohlfarth C (1988) Polydispersity effects on the demixing behavior of poly(vinyl methyl ether)/polystyrene blends. J Macromol Sci Chem A25:1055
63. Greenberg CC, Foster MD, Turner CM, Corona-Galvan S, Cloutet E, Butler PD, Hammouda B, Quirk RP (1999) Effective interaction parameter between topologically distinct polymers. Polymer 40(16):4713
64. Hill MJ, Barham PJ, Keller A, Rosney CCA (1991) Phase segregation in melts of blends of linear and branched polyethylene. Polymer 32(8):1384–1393
65. Hill MJ, Barham PJ, Keller A (1991) Phase segregation in blends of linear with branched polyethylene – the effect of varying the molecular-weight of the linear polymer. Polymer 33 (12):2530
66. Stephens CH, Hiltner A, Baer E (2003) Phase behavior of partially miscible blends of linear and branched polyethylenes. Macromolecules 36(8):2733–2741

67. Singh C, Schweizer KS (1995) Correlation-effects and entropy-driven phase-separation in athermal polymer blends. J Chem Phys 103(13):5814–5832
68. Eckelt J, Eich T, Röder T, Rüf H, Sixta H, Wolf BA (2009) Phase diagram of the ternary system NMMO/water/cellulose. Cellulose 16:373
69. Cowie JMG, McEwen IJ (1983) Polymer co-solvent systems.6. Phase-behavior of polystyrene in binary mixed-solvents of acetone with N-alkanes – examples of classic cosolvency. Polymer 24(11):1449–1452
70. Wolf BA, Willms MM (1978) Measured and calculated solubility of polymers in mixed solvents: co-nonsolvency. Makromol Chem 179:2265
71. Samadi F, Eckelt J, Wolf BA, López-Villanueva F-J, Frey H (2007) Branched versus linear polyisoprene: fractionation and phase behavior. Eur Polym J 43:4236–4243
72. Francis AW (1961) Critical solution temperatures. Advances in Chemistry Series, vol 31. ACS, Washington, D.C.
73. Eckelt J, Haase T, Loske S, Wolf BA (2004) Large scale fractionation of macromolecules. Macromol Mater Eng 289(5):393
74. Bercea M, Eckelt J, Morariu S, Wolf BA (2009) Islands of immiscibility for solutions of compatible polymers in a common solvent: experiment and theory. Macromolecules 42:3620
75. Bercea M, Eckelt J, Wolf BA (2009) Vapor pressures of polymer solutions and the modeling of their composition dependence. Ind Eng Chem Res 48:4603